Ref: Aşıkoğlu A., Vasconcelos G., Lourenço P.B., Pantò B. (2020) Pushover Analysis of Unreinforced Irregular Masonry Buildings: Lessons from Different Modeling Approaches, Eng Struct. doi: 10.1016/j.engstruct.2020.110830

PUSHOVER ANALYSIS OF UNREINFORCED IRREGULAR MASONRY BUILDINGS: LESSONS FROM DIFFERENT MODELING APPROACHES

Abide Aşıkoğlu[*1a], Graça Vasconcelos[1b], Paulo B. Lourenço[1c], Bartolomeo Pantò[2d]

Abstract

The present paper addresses the seismic performance of a half-scale two-story unreinforced masonry (URM) building with structural irregularity in plan and in elevation. The main objectives are (i) to understand the seismic response of URM buildings with torsional effects, and (ii) to evaluate the reliability of using simplified approaches for irregular masonry buildings. For this purpose, nonlinear static analyses are carried out by using three different modeling approaches, based on a continuum model, beam-based and spring-based macro-element models. The performance of each approach was compared based on capacity curves and global damage patterns. Reasonable agreement was found between numerical predictions and experimental observations. Validation of simplified approaches was generally provided with reference to regular structures but, based on the differences in the base shear capacity found here, it appears that structural irregularities are important to be taken into account for acquiring higher accuracy on simplified methods when torsion is present.

Keywords: Unreinforced masonry, nonlinear static analysis, macro-element model, equivalent frame model, finite element methods.

[1] ISISE, Department of Civil Engineering, University of Minho, Azurém, 4800-058 Guimarães, Portugal
[2] Department of Civil and Environmental Engineering, Imperial College of London, SW7 2AZ, London, UK
[a] Ph.D student, [b] Assistant professor, [c] Full professor, [d] Post-doc researcher
* Corresponding author
E-mail: abideasikoglu@hotmail.com

1. INTRODUCTION

Unreinforced masonry (URM) construction typology is widely used in construction practice and constitutes a significant portion of the building stock as residential or commercial buildings in both developed and developing countries [1]. Figure 1 intends to show the proportions of the masonry buildings in several countries. It can be observed that a vast majority of building stock in Pakistan (93%), Mexico (76%), Peru (73%) followed by Italy (62%) is composed of URM buildings which can be categorized as existing and modern buildings. The former typology usually consists of historical masonry buildings, made of stones or weak bricks with significantly large wall thickness and weak connections between orthogonal walls. They generally show local seismic behavior due to existence of flexible diaphragms weakly connected to the walls [2,3] . On the other hand, the modern buildings are characterized by regular brick-masonry configuration with limited wall thickness. Furthermore, design of the modern URM buildings require rigid floors and strong floor-to-wall connections to ensure that the global seismic response is achieved through box-behavior [4]. Although it is a sustainable construction solution owing to its thermal and acoustic efficiency, fire resistance, durability, and simple construction technology, globally masonry has been losing market share. The main reason for this is the appearance of other alternative solutions for low to medium-rise buildings, such as reinforced concrete or steel, which have relatively lower seismic vulnerability comparing to the masonry buildings in seismic areas. However, masonry construction is still extensively present in seismic prone zones [5,6]. Past seismic events showed that the seismic vulnerability of unreinforced masonry structures is high due to its low tensile strength, low ductility, and low energy dissipation capacity, particularly in the case of existing buildings lacking “box-type” behavior [7–10]. The lack of seismic design rules for URM buildings, which have been often designed mostly for vertical loads, also contributes to the high seismic vulnerability. In this regard, many research studies have been carried out in order to improve masonry structural systems under seismic actions and develop guidelines and tools for their seismic design [11–15].

It is known that nonlinear dynamic analysis is the most accurate approach to simulate and assess the seismic response of a structure [16,17]. Nevertheless, its application in engineering practice is complex and requires high computational cost, time, and a high level of knowledge for the calibration of the cyclic constitutive laws and the interpretation of the results. Response of structures is highly dependent on the seismic input used in the dynamic analysis. Furthermore, there is a lack of standardized verification procedures, in other terms, the evaluation of the seismic response of a building from the output of dynamic analysis is not straightforward. Yet, linear elastic analysis does not represent the behavior of the masonry building since the material response is highly non-linear regardless of low level of loading. Therefore, nonlinear static (pushover) analysis has been often preferred for the seismic design/assessment of structures [18]. A pushover curve provides fundamental information about the seismic performance of buildings and is a powerful tool to evaluate the seismic behavior based on displacement-based strategies. According to the displacement-based design approach, it is needed to

define seismic performance levels, which are associated with a level of damage exhibited by the structures and are commonly identified by means of strains or drift limits [19,20]. These are directly related to deformation, obtained for certain seismic intensity. According to past research, the application of the displacement-based design to masonry structures is not straightforward, and the same has been mostly applied on frame systems, such as reinforced concrete and steel buildings [21–24]. Thus, further investigation is required to adopt pushover analysis in a more systematic strategy for masonry structures with box behavior, particularly for buildings with structural irregularities to consider torsional effects imposed by its own configuration under seismic actions [19,25,26]. Such consideration is crucial because the seismic design and analysis codes are directed to regular structures whose dynamic behavior is governed mostly by translation, and they do not represent the response of the structural systems with irregularities [25].

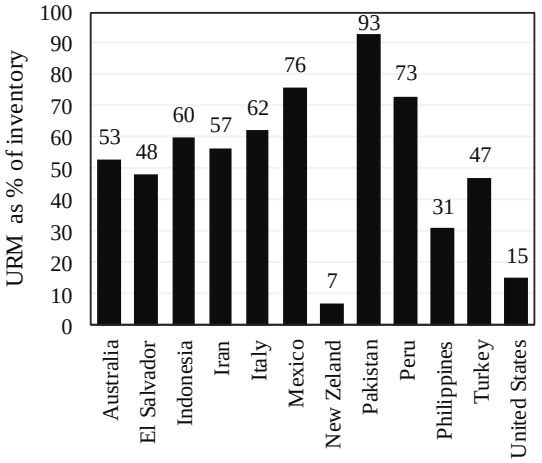

Figure 1. URM buildings in Global Building Inventory [1]

Within this framework, it is important to define appropriate modeling strategies to perform nonlinear analysis of URM buildings under seismic actions. Advanced computational applications regarding the nonlinear behavior of masonry are commonly focused on the finite element method (FEM), such as [27–32], and, also, block-based models, in which the real masonry arrangement (units and mortar) is considered [33–40]. Such analyses require a high computational effort and are complex and expensive to be adopted in practical applications. Therefore, more simplified analysis tools for masonry buildings are required.

Simplified numerical approaches, based on macro-elements, have the capability to simulate the seismic response of the masonry structures with significantly lower computational effort. It is important to note that "simplified approach" represents the methodology in which a set of assumptions taken account to describe the geometric configuration and discretize the structural elements in a simplified way. However, macro-element models are, as well, relatively complex besides allowing users less computational time. The aim of these simplified approaches is not only to provide an assessment of the ultimate strength of the structure but also, a sufficient detailed description of its nonlinear behavior by means of simplified discretization of the structural layout. Thus, they are proposed as an alternative

method for practitioners. Several simplified numerical strategies have been developed for masonry buildings, both in presence of deformable (existing buildings) or rigid diaphragms (modern buildings) to be used in general engineering practice and displacement-based design, such as the Discrete Macro Element Model (DMEM) [41] implemented in the 3DMacro [42] software and the equivalent frame model [43] implemented in the Tremuri software [44–46]. It is worth to pointing out that an important prerequisite for apply these simplified approaches is the presence of floor actions due to the presence of diaphragms, although deformable. In absence of diaphragm, different approaches, able to simulate the out-of-plane failure of masonry walls, should be employed.

Recent studies have shown that these simplified numerical approaches simulate the seismic response of buildings with reasonable accuracy. It is noticed that there is a growing interest in the scientific community in comparing different numerical approaches [47–49]. Marques and Lourenço (2011) [50] compared different macro-element models, namely the equivalent frame SAM model proposed by Magenes and Della Fontana (1998) [51] and the DMEM, as an alternative practical and reliable structural analysis tool for two-story masonry buildings. Pantò et al. (2017) [52] improved the 3D macro software developed by Caliò et al. (2012) [41] to simulate the combined in-plane and out-of-plane behavior of masonry walls. Chácara et al. (2018) [53] conducted a study aiming at the simulation of dynamic shaking table tests on a U-shaped masonry wall by means of the macro-element modeling. Bondarabadi (2018) [54] used the equivalent frame model implemented in Tremuri software [43] to validate the seismic behavior of two masonry structures tested on a shaking table by performing nonlinear dynamic analysis.

Aiming at assessing the performance of different modelling strategies for the nonlinear analysis of irregular masonry buildings in plan and elevation, the present paper presents the calibration of different numerical models, namely a continuum model and two different simplified approaches (the DMEM and the equivalent frame model), based on the results obtained in dynamic tests on the shaking table of a half-scale two-storey asymmetric URM building. A comparative analysis of the results obtained by the different models is provided. Furthermore, a sensitivity analysis is carried out by means of the simplified numerical approaches regarding key mechanical parameters, namely modulus of elasticity, and tensile, compressive, and shear strength.

2. MODELING METHODS FOR MASONRY BUILDINGS

A literature review on the methodologies applied in the seismic assessment of masonry buildings, [55], discusses different modeling approaches. Besides, [56] discusses the applicability of the available analytical tools so as to enhance the design practice of new masonry structures and as well as prevention of the historical ones. The most advanced methodology is the finite element method which allows simulating the behavior of masonry structures with accurate results. However, the method requires high computational effort, complex constitutive material laws and users with postgraduate knowledge, and,

therefore, its application in engineering practice is limited. In this regard, simplified computational tools have been proposed, based on structural components such as beam-type and panel elements.

The seismic behavior of modern masonry buildings is governed by box-behavior where the in-plane structural walls controls the resistance and premature out-of-plane mechanisms are prevented. Yet, once proper measures are taken for existing masonry buildings, the so-called box-behavior can be also achieved. Typically, the in-plane resisting mechanisms of masonry piers can be generally characterized by three modes of failure [57], as shown in Figure 2. There are several factors affecting the failure mechanisms, such as the wall geometry, quality of the masonry materials, boundary conditions and loading configurations acting on the walls. Sliding shear failure is characterized by the development of horizontal cracks when the pier has poor mortar quality and subjected to very low vertical loading. Depending on the relative resistance of units and mortar, diagonal cracking can develop along the unit-mortar interfaces as stair-stepped patterns or can develop through units and mortar. In the first case, cracking occurs when the shear strength of the unit-mortar interfaces is lower than the shear stress induced by horizontal loads. In the second case, diagonal shear failure occurs as a result of excessive tensile stresses and limited tensile strength of masonry units. This results in different resistance criteria describing the shear resistance of masonry piers. The flexural failure is mostly associated with the rocking of the walls in which crushing of the bottom corners under compressed regions and overall stability result in loss of bearing capacity of the masonry wall.

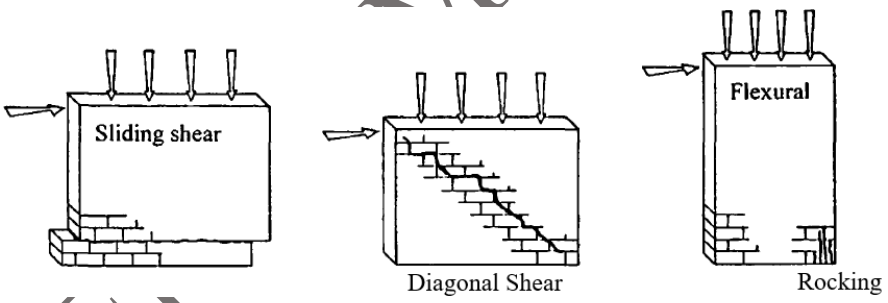

Figure 2. Typical failure modes of unreinforced masonry piers subjected to in-plane loading [57]

Since the nonlinear behavior of modern URM buildings is usually governed by in-plane resisting mechanisms, most of the proposed assessment approaches rely on resistance criteria associated only with the in-plane behavior of masonry walls. In fact, in-plane failure mechanisms play a key role in the macro-modeling approach, assuming that local failure mechanisms are prevented and global behavior of the masonry is ensured [58,59]. Methods developed for masonry buildings with box behavior may not be suitable for existing masonry buildings, in which diaphragmatic action of the floors is often compromised. The macro-element modeling approaches can be categorized into two groups, namely: (i) equivalent frame models, where the walls are represented by rigid nodes and deformable elements, as shown in Figure 3 (for instance, SAM, Tremuri model); (ii) plane macro-elements, in which walls are represented by plane or three-dimensional elements (such as variable geometry, multi-fan panel, strut-and-tie model or, macro-elements with spring links), as shown in Figure 4.

The POR method was proposed by [60] and the methodology is known as the first seismic assessment tool for masonry structures. The approach assumes a story failure mechanism and analyses each structure level individually. The nonlinear behavior of the structure is computed by taking into account the inter-story shear force-displacement curve in which the sum of the individual response of each wall is represented. The application of the method is limited to the assessment of masonry structures with a rigid diaphragm that ensures the inhibition of out-of-plane failure. Therefore, the failure of the building is based on the shear failure of the pier panels having elastic-perfectly plastic behavior with limited ductility.

The equivalent frame model implemented in Tremuri computer program [43] is based on the subdivision of the masonry walls into deformable elements (macro-elements), representing pier and spandrel components, and rigid nodes (Figure 3(a)). The deformable macro-elements concentrate the nonlinear response of the walls and are composed of three parts: the central body replicates the in-plane shear deformation and two outer elements at the top and bottom of the central body replicate in-plane bending and axial behavior. The rigid nodes correspond to the parts of the wall which do not experience damage, being only used to connect the deformable elements. The nonlinear description of the material involves a stress-strain cyclic relation with no-tension. Each macro-element has eight degrees of freedom (DOF): (a) the central body has two DOFs (horizontal translation and rotation); (b) the outer top and bottom elements present three DOFs each (vertical and horizontal translation and one rotation) (Figure 3(b)).

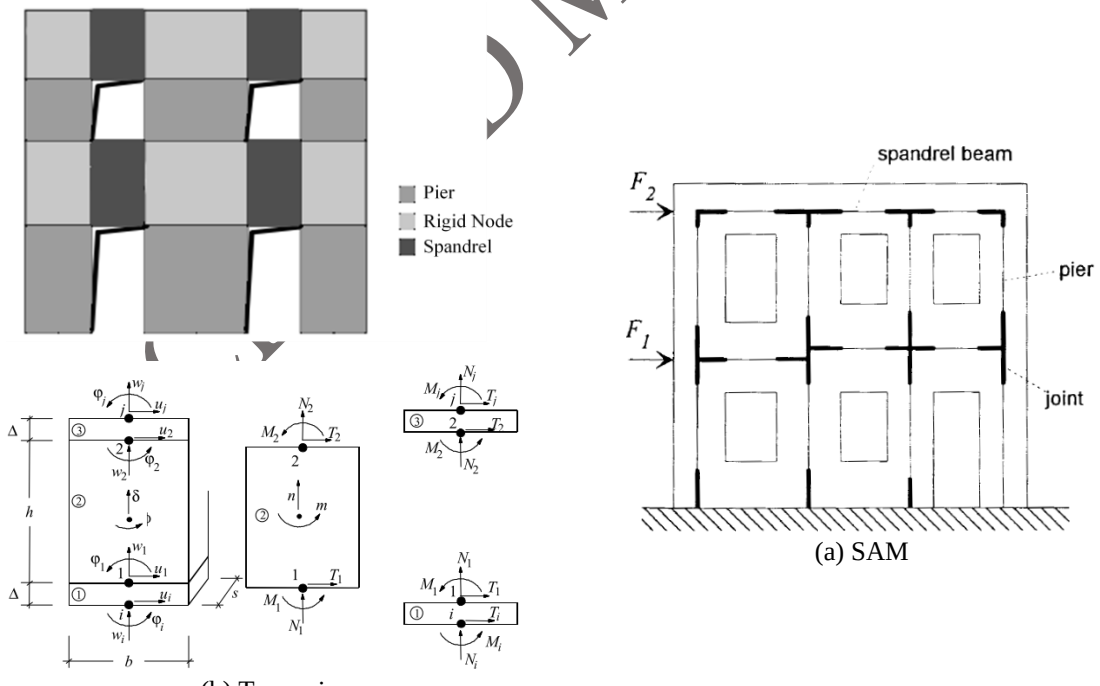

(a) SAM

(b) Tremuri

Figure 3. Beam-based macro-element models, i.e. equivalent frame models, (a) Tremuri [43], (b) SAM [51]

The Simplified Analysis of Masonry Buildings (SAM) tool was developed by Magenes and Della Fontana (1998) [51] and is based on an equivalent frame idealization of the masonry walls by means of

deformable (piers and spandrels) and rigid (joints) macro-elements as shown in Figure 3(b). The nonlinear behavior of the pier elements is governed by elastic-perfectly plastic behavior with limited ductility, whereas spandrels are considered to have either elastic-plastic or elastic-brittle behavior. The configuration of the openings in vertical alignment plays an important role to simplify the masonry wall as an equivalent frame, requiring regular distribution.

The variable geometry approach assumes that the nonlinear response is simulated by geometrical nonlinearity of the deformable macro-elements rather than material nonlinearity, aiming at analyzing multi-story walls [61]. This macro-element is composed of triangular finite elements as illustrated in Figure 4(a), and there are two types of geometric configurations, which are defined as deformable and rigid elements. The response is calculated at each load step based on the deformation observed in the shape of each triangular finite element on the resistant portions of the elements. The geometry of the rigid macro-elements remains constant regardless of the applied load, and masonry parts that are damaged or under tensile stresses are not taken into account in the calculation. The deformable parts are updated through the translation of the joints while the stress of the elements is changed while conserving the resultant force constant at each load step.

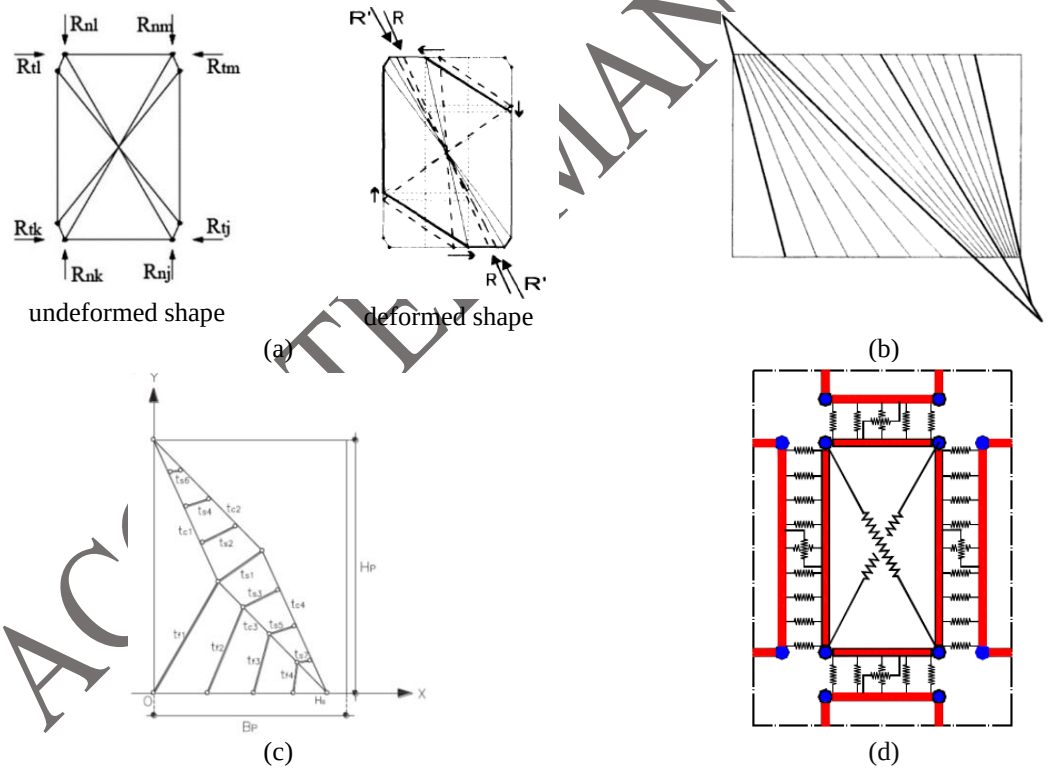

Figure 4. Panel macro-element models, (a) variable geometry [61], (b) multi-fan panel element [62], (c) strut-and-tie [63], (d) spring-based macro-element [41]

Braga and Liberatore (1990) [62] suggested the discretization of masonry buildings by means of panel elements in which a multi-fan stress pattern develops, as shown in Figure 4(b). Each macro-element is represented by two lateral edges having two rigid surfaces. Linear elastic behavior is considered for compression and zero tensile strength is assumed. Failure is identified by the crushing of the material

when reaching the maximum compressive stress. It is noted that this approach is not capable of capturing material degradation [64].

In the strut-and-tie method, the masonry building is subdivided into stories, and the vertical elements are represented by masonry panels acting as in-plane resisting elements, which are analyzed individually by means of pushover analysis [63]. The capacity curve of the story is calculated by the addition of the capacity curves obtained for each panel of that story. Hence, the capacity of the building is obtained taking into account the capacity curves of all the stories. Elasto-plastic compressive behavior and no-tension behavior are assumed. Each masonry panel is composed of an equivalent strut-and-tie member, so-called evolutive strut-and-tie, whose response is updated at each load step, allowing to investigate the response in uncracked, cracked and softening states. The geometrical shape of the strut-and-tie is changed by the decrease in the number of resisting trusses. The behavior of the masonry panel from uncracked condition to failure is simulated by the elimination of the trusses that connect the rhomboid to the base and inside of the rhomboid (Figure 4(c)), being possible to reproduce the flexural and shear failure modes, respectively. Two major simplifications are made: (i) there is no interaction between the stories and each story is analyzed individually; (ii) the panel elements only represent masonry piers and the columns, without spandrels.

A plane macro-element model, the DMEM, was proposed by Caliò et al. (2012) [41] and the generic masonry wall is obtained by assembling quadrilateral *(panel)* elements with four rigid edges and a diagonal link. Each side of the panel interacts with other panels by means of nonlinear links, so-called interfaces. The simulation of the failure mechanisms is governed by the nonlinear links at the panel and interfaces: (a) discrete distribution of orthogonal links at the interface element simulates the masonry axial/flexural behavior; (b) a single link located parallel to the interface's direction governs the shear-sliding mechanism; (c) the diagonal panel link, is responsible for the simulation of the shear-diagonal failure. Each plane macro-element includes 4 degrees of freedom, see Figure 4(d): 1 DOF to represent the in-plane deformability (diagonal spring) and 3 DOFs to describe the rigid body motions.

3. EXPERIMENTAL RESULTS

The main objective of this work is to discuss the performance of numerical models simulating the seismic behavior of irregular masonry buildings. For this purpose, the results of dynamic shaking table tests carried out on a concrete block masonry building were adopted [12]. The idea is to compare the pushover curve and numerical damage patterns with the monotonic experimental response envelop and experimental damage patterns. Shaking table tests on modern masonry buildings having symmetric [65] and asymmetric structural configuration [12] were carried out in order to investigate the influence of the torsional behavior induced by irregular geometries. It is noted that torsional behavior is present even in regular geometries after the development of nonlinear behavior and the accumulation of damage [65]. In addition, irregular structural configurations of buildings with box-behavior (presence of rigid floor

diaphragms) are intended to be analyzed since simultaneous in-plane and out-of-plane deformations may occur due to torsional effects in the post-peak regime [12].

3.1. Description of the Concrete Block Masonry Building Model

The experimental model was designed based on typical modern masonry houses built in Portugal and encompassing the Eurocode 8 [66] criteria for: (i) bi-directional resistance and stiffness, (ii) torsional resistance and stiffness, and (iii) diaphragm behavior of the slabs. The experimental model is an irregular building in plan, which has a setback in one corner and has an irregular distribution of openings in elevation. In order to achieve more representative response from the half-scale experimental model, both Cauchy and Froude similitude laws should be respected [67]. As per Froude similitude law, additional masses are required. However, limitations of the shaking table, i.e. pay load, did not allow the implementation of both, and, therefore, only Cauchy's similitude law was adopted (Table 1) [12]. The masonry walls are composed of concrete block units and are connected to reinforced concrete slabs. The units are laid in running bond configuration allowing interlocking at the wall intersections. An experimental campaign was carried out in order to characterize the properties of the materials, i.e. mortar, brick unit, and masonry panel. The results of the characterization tests are summarized in Table 2. The experimental building has 4.2 m x 3.4 m in plan and 3.0 m height, whereas the slab and wall thickness is 0.1 m. The typology of the RC slab is two-way with reinforcements of Ø8//15. The height of each level is 1.4 m having window and door openings with 0.8m x 0.5m and 0.5 m x 1.1 m, respectively (Figure 5). Additionally, RC lintels were constructed above the openings. The total weight of the experimental model is nearly 110 kN in which 58% of the weight belongs to the slabs and following what was mentioned before it does not include additional masses. Furthermore, the wall without any opening (south wall) represents the common wall shared in twin house configurations. The structure was constructed on a RC ring-beam slab foundation with dimensions of 4.9 m x 4.4 m x 0.35 m.

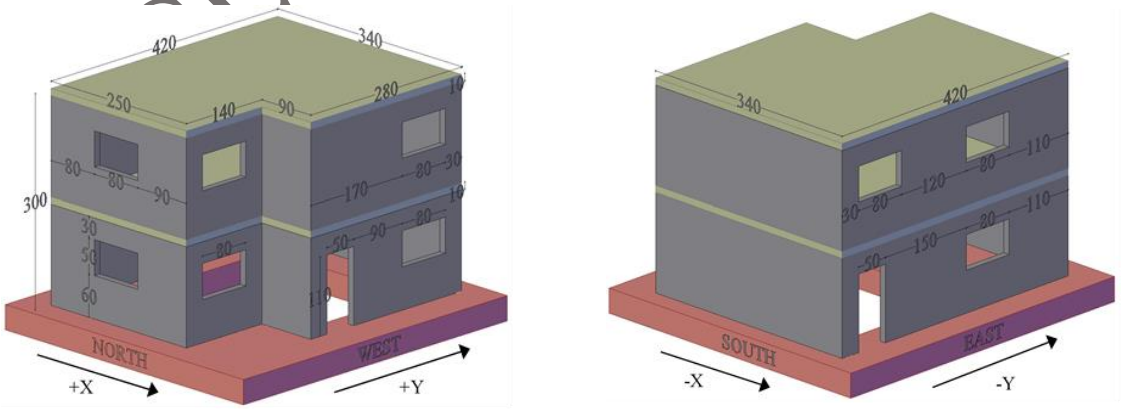

(a) (b)

Figure 5. The structural configuration of the URM building, (a) north-west façade, (b) south-east façade [16]

Table 1. Scale factors used for Cauchy's similitude law [67]

Parameter	Symbol	Relation Prototype/Model	Cauchy scale factor
Length	L	L_P/L_M	λ
Young's Modulus	E	E_P/E_M	1
Specific mass	ρ	ρ_P/ρ_M	1
Area	A	A_P/A_M	λ^2
Volume	V	V_P/V_M	λ^3
Mass	m	m_P/m_M	λ^3
Displacement	d	d_P/d_M	λ
Velocity	υ	υ_P/υ_M	1
Acceleration	a	a_P/a_M	λ^{-1}
Weight	w	w_P/w_M	λ^3
Force	F	F_P/F_M	λ^2
Moment	M	M_P/M_M	λ^3
Stress	σ	σ_P/σ_M	1
Strain	ε	$\varepsilon_P/\varepsilon_M$	1
Time	t	t_P/t_M	λ
Frequency	f	f_P/f_M	λ^{-1}

Table 2. Material properties obtained by experimental campaign [16]

Mortar	
Flexural strength	2.70 MPa
Compressive strength	11.71 MPa
Block	
Tensile strength	3.19 MPa
Young's modulus	9.57 GPa
Compressive strength	12.13 MPa
Masonry Panel	
Young's modulus	5.30 GPa
Compressive strength	5.95 MPa
Shear strength	0.12 MPa
Shear modulus	1.76 GPa

3.2. Test Procedure and Results

The seismic input load for the shaking table was introduced by using two artificial accelerograms in the longitudinal (Y) and transversal (X) direction. The accelerograms were derived based on the elastic response spectrum provided in Eurocode 8 [66] considering the design ground acceleration of Lisbon region, which is 1.5 m/s^2 (0.15g), ground type A, type 1 seismic action and 5% damping. The artificial accelerograms were scaled by a factor of 2 (compressed in time and multiplied in acceleration) and applied as reference input (Figure 6). The seismic response was achieved by applying the seismic load in phases with increasing intensity, thus scaling the reference seismic input. The sequence of the seismic input and corresponding intensity in terms of peak ground acceleration (PGA) are presented in Table 3. A total number of 6 test runs was considered and, therefore, cumulated damage was measured due to the sequential seismic input.

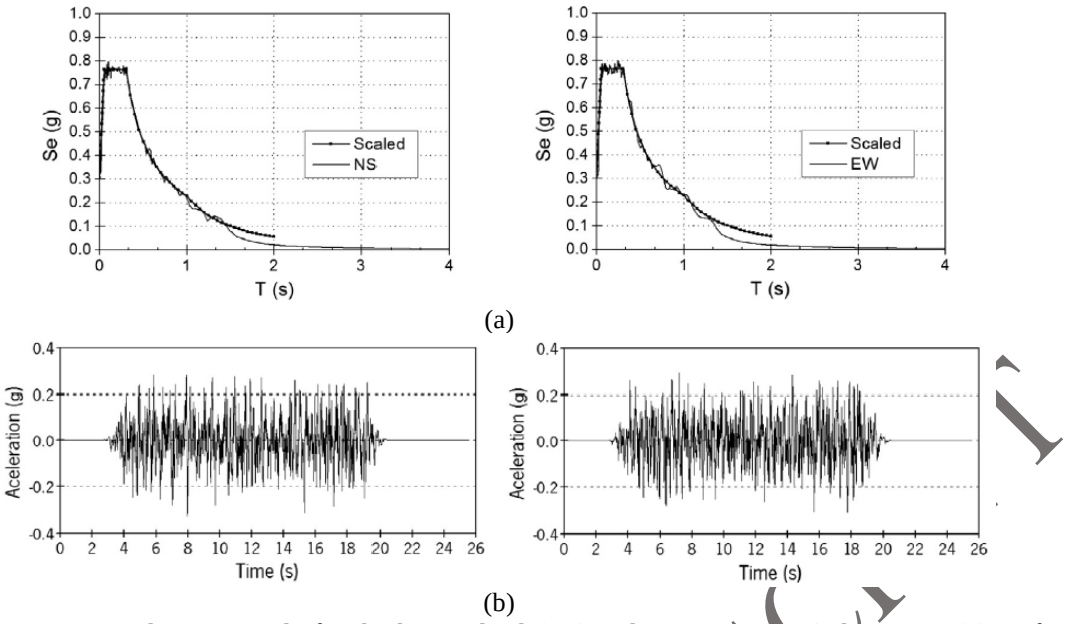

Figure 6. Input signals at 1:2 scale for the longitudinal (NS) and transverse (EW) directions: (a) artificial response spectrums, (b) acceleration-time series [16]

Table 3. Seismic input series and corresponding PGA [16]

No.	Test	PGA NS (m/s2)	PGA EW (m/s2)
1	25%	1.16 (0.12 g)	0.89 (0.09 g)
2	50%	2.50 (0.26 g)	2.31 (0.24 g)
3	75%	3.25 (0.33 g)	2.79 (0.28 g)
4	100%	4.57 (0.47 g)	4.05 (0.41 g)
5	150%	6.45 (0.66 g)	10.46 (1.07 g)
6	150% 2	6.44 (0.66 g)	12.19 (1.24 g)

A detailed description of the damage patterns based on visual inspection after each test run was presented in Avila (2014) [16]. For the first test run (25%, 0.12g), no significant damage was reported. The first minor damage was observed around the window openings as stepped cracks after the input 50% (0.26g). The third test run, which corresponds to 75% (0.33g) of the reference input, resulted in significant horizontal cracks at both levels. Additionally, diagonal stepped cracks were identified connected to the horizontal cracks concentrated on the first floor. Increasing seismic input to 100% (0.47g) led to a moderate increase in displacements, and, development of new horizontal and diagonal cracks mainly concentrated on the north and west walls. At the end of the test run 150% (1.07g), the state of the imminent collapse was achieved due to severe damage in the URM model. A significant increase in the displacement values was observed in all walls, particularly the transversal ones. According to Avila (2014) [16], although the out-of-plane displacements were relatively very low with respect to in-plane displacements, higher values were obtained in the second level of the building. This imposed large deformations in that story and an extension of the cracks from the previous test run and the onset of horizontal and diagonal cracking was reported in the south and east walls. It is possible to conclude that torsional effects were developed not only due to plan irregularity but also due to irregular locations of

the openings and previous damage. Figure 7 presents the damage pattern observed in the URM model at the end of the dynamic test. Accordingly, an envelope curve of the hysteretic response was developed through the maximum base shear and maximum displacement of the hysteresis loops after each test run.

(a) (b)

Figure 7. Damage observed after the final input sequence, (a) north wall, (b) west wall [16]

4. NONLINEAR NUMERICAL ANALYSIS

The numerical investigation of the seismic behavior of the masonry building (experimental model) was carried out by using three different approaches, namely spring-based macro-element (DMEM), beam-based macro-element (equivalent frame) and continuum modeling. For this purpose, practice-oriented software 3DMacro and Tremuri were considered together with a continuum model constructed in DIANA FEA (Figure 8). It is important to notice that continuum models represent the mechanical response of the masonry at the scale of the material while macro-element models simulate the response at the scale of the panel (walls). According to their simplified modeling strategy and in order to guarantee a low computational effort, a refined mesh is not required in the case of macro-element models. The mesh discretization was carried out with 800 mm elements with a total number of 827 degrees of freedom in 3DMacro. The equivalent frame model discretization in Tremuri allows representing the model with only 63 elements having a number of 78 DOFs. In DIANA FEA, a three-dimensional continuum model was prepared with solid brick elements (CHX60) having a mesh size of 100 mm. Although solid elements require high computational effort since the number of degrees of freedom are increased, solid elements were preferred rather than shell ones. The main aim to simulate the plastic deformations along the masonry thickness and simulate better the out-of-plane contribution of the walls to the global response. The continuum model assumes the masonry as homogeneous continuous material behavior, as Lourenço (2002), [69] and, is composed of 6574 solid brick elements with a total number of 138,048 degrees of freedom.

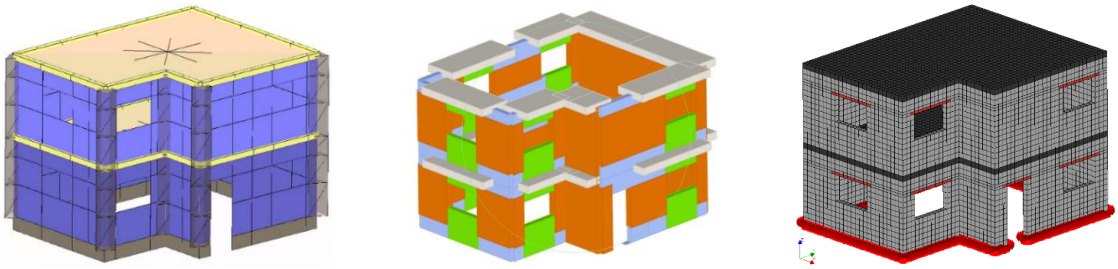

(a) (b) (c)

Figure 8. Numerical models constructed by using different approaches, (a) spring-based macro-element modeling in 3DMacro, (b) beam-based macro-element modeling (EFM) in TREMURI, (c) continuum modeling in DIANA FEA

4.1. Calibration of the Linear Properties

The calibration of the numerical models based on the constitutive laws obtained from in-plane loaded masonry panels would be more accurate [70,71]. However, due to the absence of this data, it was decided to proceed with the calibration of the numerical models through the fitting of the initial stiffness in the linear range of nonlinear pushover curves and, thus, the mechanical property involved in the calibration process was the modulus of elasticity masonry (E). The modulus of elasticity obtained experimentally by Avila (2014) [16] was 5300 MPa. However, this value needed to be reduced to reflect cracking of the concrete block masonry during transportation before the test, and accumulation of microcracks in the first loading stages during the shaking table tests. It must be stressed that the modulus of elasticity used in the three numerical approaches differs due to modeling assumptions in each software. An isotropic continuum behavior is considered for the continuum model which allows the definition of the elastic parameters, such as E and G, having a dependency to each other by the relationship $G=E/(2+2\gamma)$. On the other hand, microelement models generally assume uncoupled relationship between E and G parameters. This is an inconsistency between the modeling approaches, which poses questions on the reliability of displacement-based seismic assessment approaches for irregular masonry buildings, given their higher dependency on the elastic properties.

In theory, the stiffness of a wall in linear range is only dependent on the modulus of elasticity of masonry, the geometry of the panel and boundary conditions. However, various experimental studies proved that initial stiffness is influenced also by pre-compression load level significantly [72–75]. According to Araújo (2014) [74], the numerical simulation of the elastic parameters requires an equivalent modulus of elasticity by means of calibration. Thus, experimental value of the modulus of elasticity obtained in small masonry wallets under uniaxial compression may not be representative of a masonry wall. In fact, it is stressed that a precise description of numerical models for masonry buildings requires certain hypothesis. In the particular case of continuum models, it is important to recall that significant assumptions have been made, namely (i) masonry (concrete block, mortar and unit-mortar interfaces) considered as an homogenous material and (ii) full fixed connection between the structural components. Once all methodologies adopt macro nature of masonry, the discrepancy in elastic modulus can be associated to the features of modeling approaches, i.e. connections of intersecting walls (flange

effect). With this respected, it is important to stress that (i) the continuum model assumes fully fixed connection along the height, (ii) the equivalent frame model considers lumped rigid nodes at the story level, as already discussed by Simões (2018) [76], and (iii) discrete macro-element model only shares the vertical deformation at the intersections. Therefore, aiming at clarifying the need for adopting different values of modulus of elasticity among the different modelling approaches, a simple benchmark study was carried out.

4.1.1. Benchmark study on the modulus of elasticity.

Firstly, to what concerns the linear elastic properties of the models, two in-plane loaded masonry panels with different geometry subjected to 0.5 MPa pre-compression were analyzed considering three approaches. An experimental campaign on cyclic behavior of masonry panels, which was carried out by [77], was considered and one level of pre-compression was selected for one slender (h/l=2) and one squat (h/l=1) wall. All specimens have a thickness of 0.32 m and a height of 2.5 m while the length of the slender (CS01) and squat (CT01) specimens are 1.25 m and 2.5 m, respectively. Furthermore, continuum model was constructed and analyzed by [74] in Diana FEA. It is noted that linear properties were calibrated with respect to experimental shear tests. The mechanical properties defined for continuum calibrated models are gathered in Table 4.

Table 4. Mechanical properties for masonry in calibrated continuum models [74]

	E (MPa)	γ (kg/m^3)	f_c (MPa)	G_c (N/mm)	f_t (MPa)	G_t (N/mm)
CS01	1500	1900	3.28	5.25	0.14	0.02
CT01	1000	1900	3.28	5.25	0.14	0.02

Within the scope of benchmark, simulation of experimental campaign was carried out using both macro-element models by means of pushover analysis. Material properties assigned for masonry are listed in Table 5 and force-displacement curves are shown in Figure 9. It is clearly seen that the need for different modulus of elasticity values among different approaches is crucial to investigate on structural level. The main idea was to get a better insight on the influence of the flange effect of the orthogonal walls by means of corner connections. As previously mentioned, strategies adopted for the modeling of connections of intersecting walls are different for each representative model.

Table 5. Mechanical properties for masonry in calibrated macro-element models

			3DMacro Model		Tremuri Model	
			CS01	CT01	CS01	CT01
Linear Parameters	Modulus of Elasticity	E (MPa)	1500	1000	1500	1000
	Shear modulus	G (MPa)	600	400	600	400
	Specific weight	γ (kN/m^3)	1900	1900	1900	1900
Nonlinear Parameters	Tensile strength	f_t (MPa)	0.14	0.14	-	-
	Compressive strength	f_c (MPa)	3.28	3.28	3.28	3.28
	Shear strength	fv_0 (MPa)	0.16	0.10	0.16	0.10
	Friction coefficient	μ	0.30	0.30	0.30	0.30

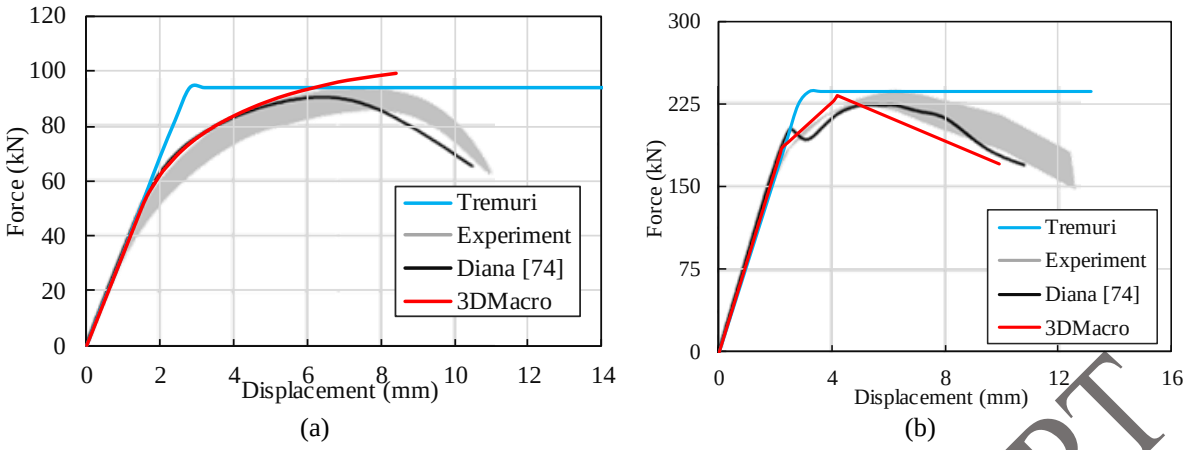

Figure 9. Force-displacement curve for, (a) CS01, (b) CT01

For this, a simple geometry was used to analyze the difference in the elastic range for the different approaches, as shown in Figure 10. Three continuum models with different connection levels at the corners were prepared such as (i) fully fixed connection; (ii) no corner connection by means of interface with zero stiffness, and (iii) no connection with calibrated modulus of elasticity of masonry. In this way, it is possible to have an insight on the role of orthogonal wall connections adopted by different approaches. The comparison is carried out in terms of linear regime of the pushover curve, elastic stiffness (roughly based on F=k.d), its variation among the models, and modal parameters in Table 6.

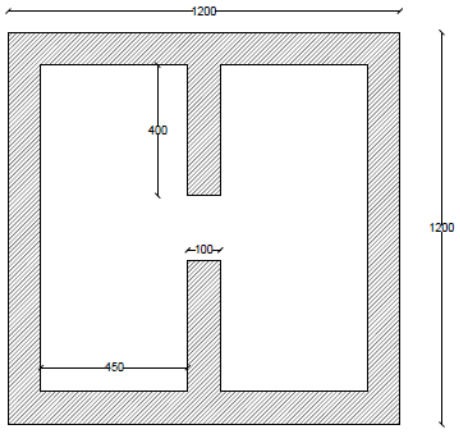

Figure 10. Structural configuration of the benchmark model, dimensions in mm (height is 1500 mm)

In Table 6, variation of elastic stiffness is listed based on three different variations. With respect to Case 1, calculations were carried out with respect to Diana Fixed model. The model with fixed corner connection is considered as reference model as it was the adopted approach for the continuum model analyzed in the case study (asymmetric URM building). It is noticed that inefficient connection of the orthogonal walls results in 20% reduction in the elastic stiffness compared to the fully fixed connections. The elastic regime (k) of Case 2 (Diana with no connection E1000) is 19% less than the elastic stiffness obtained in Case 1 (Diana fully fixed). By increasing 50% the modulus of elasticity of masonry, a lower difference (6%) in elastic stiffness is achieved. Furthermore, the similar increment is also observed in terms of modal properties, for instance the frequency of the first mode of vibration has 13% difference

in Case 2 while only 1% variation is achieved by calibration of the modulus of elasticity in Case 3. It is clearly seen that simulation of connections requires further improvement.

Table 6. Variation in the elastic stiffness (k) and modal parameters for the first mode of vibration

Case	k (LF/disp)	variation with respect to Case 1 (%)	Frequency (Hz)	Mass Participation in Y (%)	Variation in frequency with respect to Diana fixed (%)
1. Diana_Fixed	4.8	-	36.8	73	-
2. Diana_NoConnection_E1000	3.9	81	32.1	76	-13
3. Diana_NoConnection_E1500	5.1	106	36.5	76	-1

Results of the benchmark study justify the need to use different modulus of elasticity. Calibration of one numerical model with respect to experimental campaign could be necessary to be carried out for in-plane loaded masonry piers. Yet, the same mechanical properties provide good agreement among different modeling approaches, as expected. In structural level, a simulation of a complete structure is highly dependent on the modeling assumptions that influences the value of modulus of elasticity. Therefore, it was decided to select different values for the modulus of elasticity of masonry for the asymmetric URM model, according to linear properties that is summarized in Table 7.

Table 7. Linear properties adopted

			DIANA Model	3DMacro Model	Tremuri Model
Linear Parameters	Modulus of Elasticity	E (MPa)	1000	1500	2000
	Poisson's ratio	υ	0.25	-	-
	Shear modulus	G (MPa)	-	600	800
	Specific weight	γ (kN/m^3)	1200	1200	1200

4.2. Nonlinear mechanical properties

The nonlinear properties of masonry adopted in the numerical models are gathered in Table 8. In case of the macro-element models, "material constitutive laws" refers to masonry panel and not to the material and the nonlinear mechanical properties are defined based on the panel constitutive laws adopted in each approach. In case of the continuum model, mechanical properties defined refers to masonry material that is a nonlinear isotropic continuum. It is noted that macro-element models take into account the variability of the axial load during the analysis [41,78].

In the continuum model, the nonlinear behavior was described by the total strain rotating crack model that is available in DIANA FEA (2017) [79], see Figure 11. The constitutive model in tension was based on exponential stress-strain relation, while a parabolic relation for both hardening and softening was adopted for compression. The compressive strength of masonry was obtained by a uniaxial compressive test carried out on concrete block masonry wallets [16]. Similarly, the value of the tensile strength of masonry was taken as 0.12 MPa based on Avila (2014) [16]. According to Angelillo et al. (2014) [80], an average ductility index in compression (ratio between fracture energy and strength)

equal to 1.6 mm was considered to evaluate the fracture energy in compression. The fracture energy in tension was fixed as 0.012 N/mm.

In the present study, the equivalent frame model was constructed by using commercial version, but the analyses were performed through the research version of Tremuri. The research version allows to use nonlinear macro-element ("elementi command") instead of nonlinear beam element ("macroelementOPCM 3274"). In this work, beam-based approach was defined by macro-element implemented in [81]. Therefore, a bilinear constitutive model with zero tensile strength and stiffness degradation in compression with limited compressive strength is defined in Tremuri, see Figure 11(a) [82]. Degradation in compressive stiffness replicates toe-crushing phenomena under cyclic loading. The constitutive shear-global drift (v-u) law describes the sliding displacement at horizontal mortar joints to simulate diagonal cracking. Additionally, shear behavior is characterized by a plastic component of sliding displacement (s) which is activated once the Mohr-Coulomb criterion for the friction limit is exceeded (Figure 11(a)). Shear damage variable (α) is a scalar parameter that defines the shear damage [81]. At the state of elastic range, α corresponds to 0, and becomes equal to 1 when the panel reaches its peak shear strength. Hence, the post-peak softening branch begins when α is greater than 1. Thus, the mechanical properties of the masonry panel, such as shear modulus (G), initial shear strength (f_{vo}) and friction coefficient (μ), control Mohr-Coulomb yield surface. It is also required to define the slope of the softening branch (β) and shear deformability parameter for the macro-element (c_t). In the present case, the slope of the softening branch was not taken into account, and the product Gc_t was considered as one (typical ranges are 1-4, [82]). Tensile strength is automatically considered to be zero in the model.

Table 8. Nonlinear properties of the masonry material

			DIANA Model	3DMacro Model	Tremuri Model
Tensile Parameters	Tensile strength	f_t (MPa)	0.12	0.12	-
	Fracture energy	G_f^I (N/mm)	0.012	-	-
Compressive Parameters	Compressive strength	f_c (MPa)	5.95	5.95	5.95
	Fracture energy	G_c (N/mm)	9.52	-	-
Shear-diagonal parameters	Shear strength	fv_0 (MPa)	-	0.15	0.15
	Friction coefficient	μ	-	0.33	0.33
	Shear drift		-	0.06%	0.06%
	Bending drift		-	0.08%	0.08%

In the DMEM (3DMacro), the definition of the mechanical properties is based on the calibration of the nonlinear spring links located at the interfaces, along the vertical and horizontal panel edges and diagonally within the panel element. The orthotropic behavior of the masonry can be simulated by the characterization of vertical and horizontal interfaces separately. The interface transversal links, governing the axial/flexural masonry behavior, are characterized by a perfectly elasto-plastic constitutive law with different strengths and ultimate displacements in compression and tension. This constitutive law is calibrated according to an analogous stress-strain (f-ε) characterizing the masonry (Figure 11(c)), by means of calibration procedures described in [83]. The shear behavior is associated

with two types of nonlinear links because the failure mechanism can develop along the diagonal inside the macro-element and/or along the interfaces (sliding). Thus, diagonal shear behavior is simulated by the diagonal links according to an elasto-plastic constitutive law given by Turnsek and Cacovic or Mohr-Coulomb criterion. In the present case study, the latter was considered since the diagonal shear failure was mostly associated to the sliding along the unit-mortar interfaces. Furthermore, the shear-sliding response of the material was governed by a rigid-plastic behavior in which the plastic range was adjusted according to a Mohr-Coulomb law at the transversal links [83]. In the present work, the shear-sliding behavior was not taken into account in the numerical simulations, given that there are no evidences of its occurrence in the experimental model.

The properties describing the diagonal-shear behavior of masonry are the friction coefficient (μ) and initial shear strength (f_{v0}). The friction coefficient was calculated based on the recommendation provided by Mann and Muller (1982) [84], being for the present case equal to 0.33. Being the masonry composed of aggregate concrete units and general-purpose mortar from the class M10, the initial shear strength recommended by Eurocode 6 (2005) [85] is 0.2. This value was reduced to 0.15 so that the numerical pushover curve could fit the experimental monotonic envelope. This can be justified by the damage introduced and stated above. The deformation limits regarding the flexural and shear behavior were described in terms of lateral drifts, being the maximum values of 0.06% and 0.08% in shear and bending, respectively. These values were adopted in the macro-element approaches.

It should be stressed that the same diagonal shear parameters were used for the macro-element models, the same tensile strength was used for the continuum and spring-based macro-element model and the same compressive strength for all models were adopted, see Table 8.

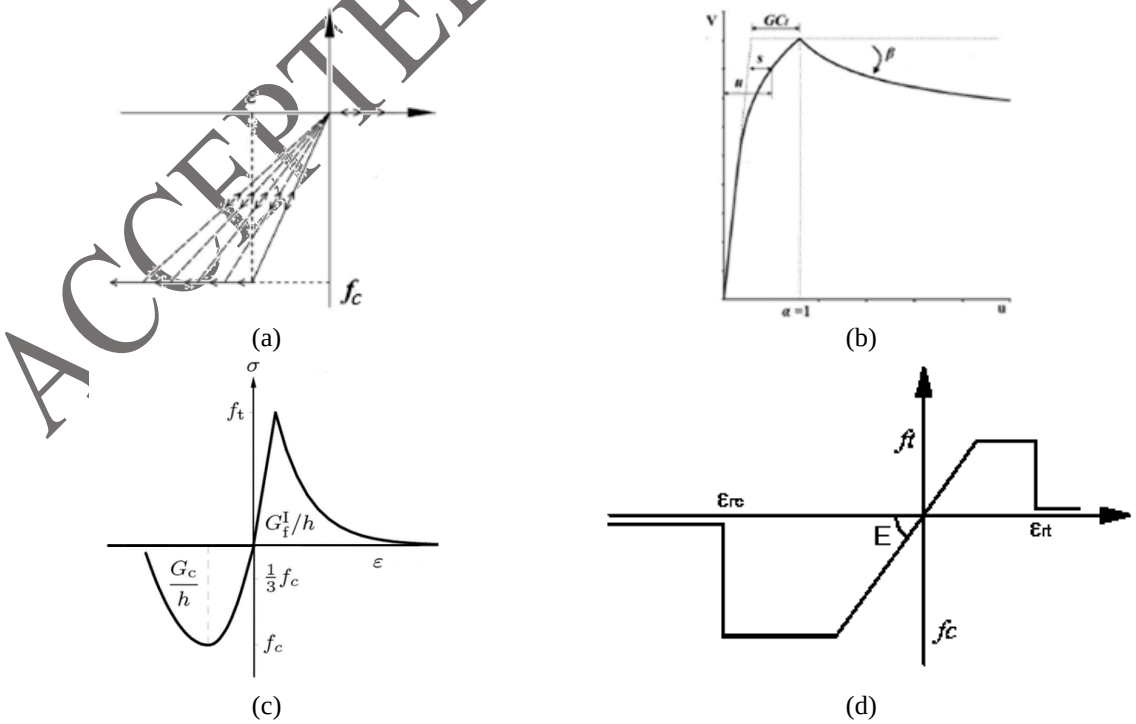

Figure 11. Constitutive material model defined in (a) Tremuri [82], (b) Tremuri for shear behavior [82] (c) Diana model [79], (d) 3DMacro [86]

5. Eigenvalue Analysis

The modal properties and mode shapes of each numerical model are presented in Table 9 and Figure 12, respectively. The mass activated for each mode along the X (M_x) and Y (M_y) directions, expressed as a percentage of the seismic mass of the model, are reported in Table 9. Finally, the total masses, in both directions are indicated in the last two columns of the same table ($M_{x,\,sum}$, $M_{y,\,sum}$). The three natural frequencies and modes shapes among the three numerical models are compared. It is found that the continuum model has a first translation mode of 13.7 Hz in the longitudinal (Y) direction, and a second mode with translation combined with torsion corresponding to a frequency of 14.4Hz. A torsional mode is observed for the third mode of vibration having a frequency of 24.0 Hz. The 3DMacro model presents the first three frequencies equal to 14.5 Hz, 15.6 Hz, and 40.3 Hz. Similar to the continuum model, the mode shapes of the 3DMacro model display translational vibration as the first mode while the second and third modes are a combination of translation and torsional rotation. In case of the Tremuri model, the first 3 frequencies obtained are 13.7 Hz, 16.9 Hz, and 22.7 Hz. The first mode presents translational motion in transversal (X) direction affected by torsional rotation, while the second mode is translational with an activated mass of 25.0% and 63.3% in X and Y directions, respectively. Again, a rotational mode of vibration was found as the third mode. In all models, the total effective mass ratio, associated with the first three modes, resulted higher than 80% in both the main directions (X and Y) of the building. It means that the higher modes do not influence significantly the seismic response of the system. Moreover, it is important to notice that significant effective mass ratios are associated with the torsion modes, confirming the important role played by the structural irregularities on determining the dynamic properties of the building.

The frequencies corresponding to the first and second modes obtained in continuum and spring-based macro-element are close being the differences of about 6% and 8%, respectively. The frequency obtained with Tremuri is close to continuum model but translational modes in X and Y directions are switched with respect to FEM and 3D macro-element and seem to be influenced by rotational components. The frequency associated to the torsional mode shape (third mode) obtained by the continuum model differs from 68% to the 3DMacro and differs from 5% to the Tremuri. Two different trends are registered: 3DMacro is stiffer than the continuum model, whilst Tremuri model provides a lower torsion stiffness than the continuum model. This poses questions on the reliability of the different approaches for time history analysis of irregular masonry buildings as the dynamic characteristics of the approaches are quite different. Moreover, given the important torsional components found, the mode-proportional distribution of inertial forces in case of irregular buildings is questionable. The differences found in the modes between the different approaches further confirm this statement. Therefore, for pushover analysis of irregular masonry buildings only uniform and inverted triangle mass distributions should be used.

476 **Table 9.** Modal properties of each model

DIANA							
Mode	**T (s)**	**f (Hz)**	**Error to f_{DIANA} (-)**	**Mx (%)**	**My (%)**	**Mx Sum (%)**	**My Sum (%)**
1	0.073	13.7	-	6.4	78.7	6.4	78.7
2	0.070	14.4	-	73.6	6.7	80.0	85.3
3	0.042	24.0	-	1.6	0.4	81.6	85.7
3DMacro							
1	0.069	14.5	6 %	0.9	88.1	0.9	88.1
2	0.064	15.6	8 %	83.8	1.1	84.7	89.1
3	0.025	40.3	68 %	0.1	5.1	84.9	94.2
Tremuri							
1	0.073	13.7	0 %	39.3	17.7	39.3	17.7
2	0.059	16.9	17 %	25.0	63.3	64.3	81.0
3	0.044	22.7	5 %	22.7	8.7	87.0	89.7

477

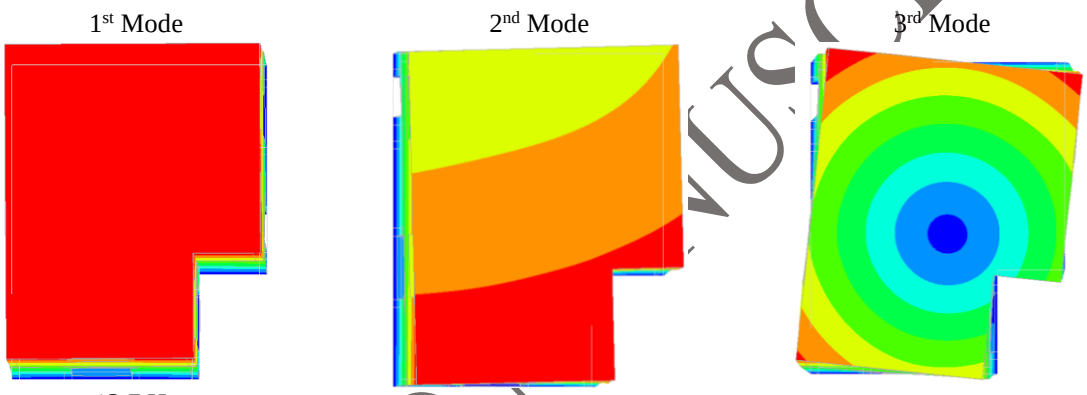

(a)

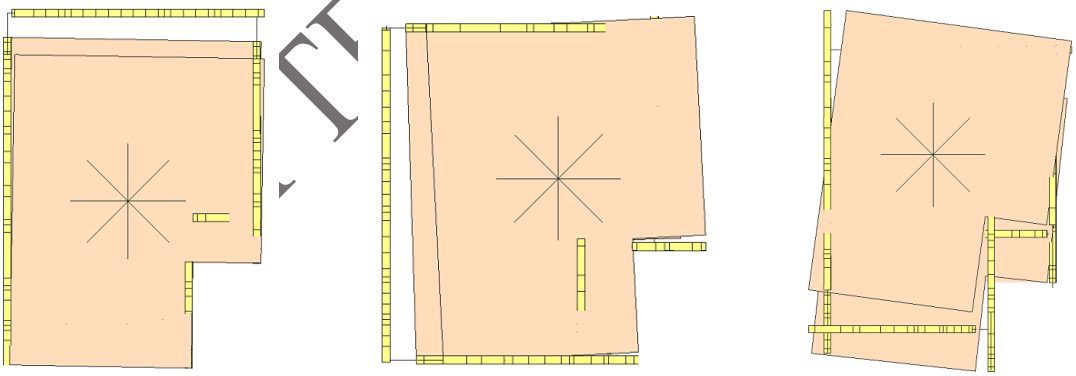

(b)

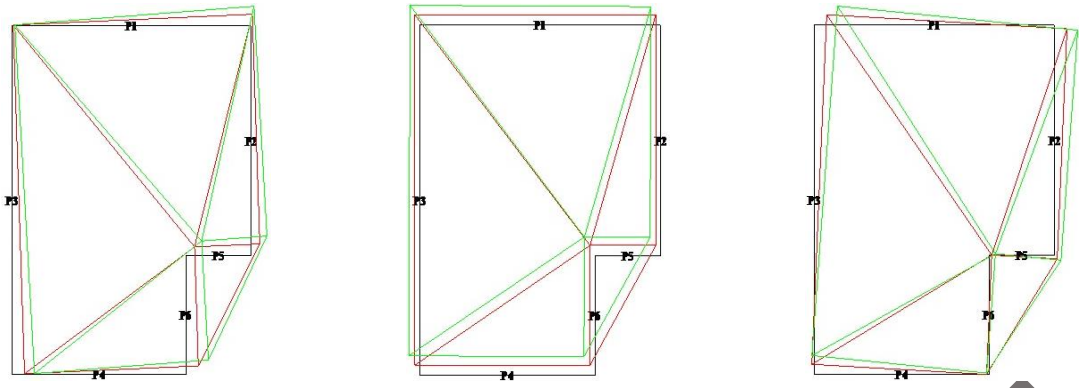

13.7 Hz 16.9 Hz 22.7 Hz

(c)

Figure 12. Modes of vibrations for the first three modes, (a) DIANA, (b) 3DMacro, (c) Tremuri

5.1. Pushover Curves

The nonlinear static analysis of the continuum model was performed by adopting the secant iterative step-solution method with arc-length control [79]. The energy norm was considered to have a tolerance of 0.001 in order to compute equilibrium at each load step. Simplified approaches do not allow any preference for the analysis options and the Newton-Raphson method is used for the iteration of the results while performing nonlinear analyses. Additionally, 3DMacro uses both force and displacement control load processes in order to obtain the post-peak branch of the capacity curve. A mass proportional (or uniform) loading pattern was considered in each direction (X and Y) to replicate the seismic loading acting on both continuum and macro-element model. The unidirectional incremental lateral forces were applied monotonically after the application of the self-weight loading of the structure. Since the masonry building ensures the box-behavior by rigid diaphragmatic action, the pushover curves are evaluated by taking a control point on the diaphragm at the top level. The capacity curves obtained for the different numerical models are presented in terms of base shear coefficient (BSC) and drift ratio at the top level of the structure. The base shear coefficient is calculated as the ratio between the base shear forces and the self-weight, and drift ratio at the top level of the structure.

In Tremuri, the masonry is assumed as zero tensile strength material [87]. It was decided to consider an additional continuum model (DIANA) and DMEM (3D macro), in which the tensile strength capacity of the masonry was also assumed as zero. This enables to have more compatible models for further comparison. Therefore, in total, five different models were prepared, three models with zero-tensile strength and two, in 3DMacro and DIANA, with a finite tensile strength.

The capacity curves obtained from the different approaches are compared with the envelope curve of the experimental hysteretic response of the building, see Figure 13. The difference between each numerical model and experimental results in terms of peak load in a positive and negative direction is calculated in terms of the maximum base shear coefficient in each direction. The difference in the peak load among the different numerical models is also calculated following the same procedure. The differences in the peak load are presented in percentage, see Table 10.

In terms of initial lateral stiffness, a slight difference in the transversal (X) direction is observed. However, it can be considered that both macro-element models are able to satisfactorily simulate the linear response of the building and are in a good agreement with the continuum model. The main reason for the difference registered in the +X direction might be due to the loading process adopted in the shaking table. Accumulation of the damage due to the phased and incremental subsequent load sets is particularly remarkable beyond the elastic behavior. This happens after the 2nd loading phase, corresponding to an input seismic load of 50% (0.26g), see Figure 13.

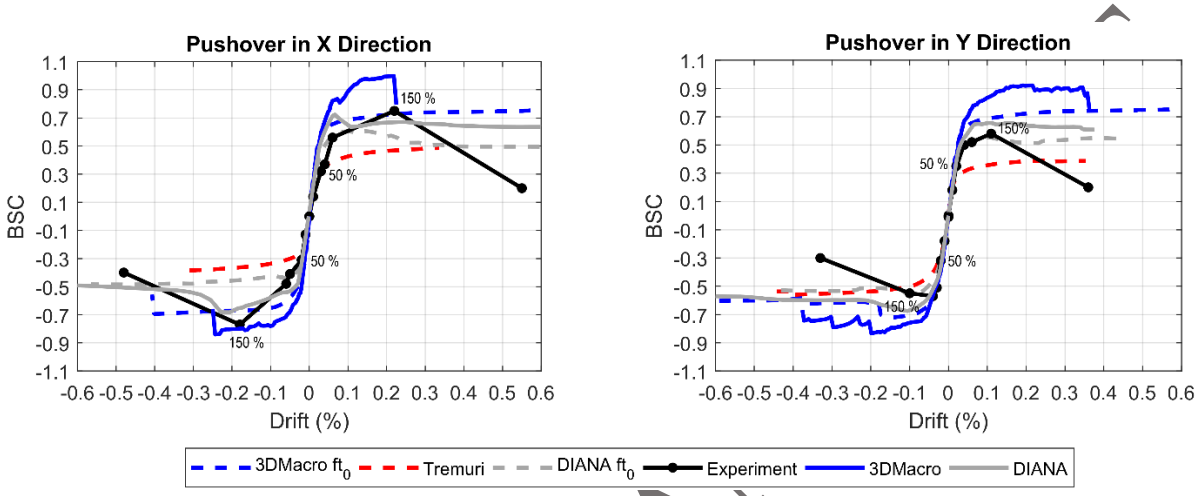

Figure 13. Capacity curves obtained from different approaches

It is also clearly seen that there is a significant difference in the maximum lateral load capacity between the experimental results and the numerical prediction obtained by the continuum model and the DMEM when finite tensile strength is considered. The macro-element model (3DMacro) achieves a shear capacity considerably higher than the capacity predicted by the continuum model (+23%) and the average experimental results (+36%). The continuum model has only a 4% difference in terms of peak load capacity comparing with the experimental one. On the contrary, the equivalent frame model (Tremuri) is conservative and has the lowest capacity against the lateral forces, presenting about less 30% than the lateral experimental load capacity. This lower capacity is attributed to the zero tensile strength considered for masonry. In fact, when zero tensile strength is considered both in the continuum model and spring-based macro-element model, the average capacity reduces, particularly in the case of the macro-element model. When zero-tensile strength is considered, the base shear capacity predicted by 3DMacro is in average 12% higher than the capacity of the experimental model. On the other hand, the value of the capacity obtained in the continuum model is now lower than the capacity in the experimental model by 16%. The difference between the load capacity recorded in Tremuri compared with the other programs is high in case of zero tensile strength, in the order of 63% in the case of 3DMacro and 22% in the case of the continuum model. This difference may be related to the limitations of the equivalent frame model discretization of masonry building with irregular opening distribution, as mentioned by Siano et al. (2017) [88]. In any case, it appears to be reasonable rely in the models with zero tensile strength in the sense that this can be an artificial procedure to take into account the cracking

accumulation due the loading phased procedure adopted in the experimental campaign. It is acceptable the previous cracking at the unit-mortar interfaces can influence the shear resistance of the masonry building.

Table 10. The difference between the results in terms of the average lateral peak load in all directions (%)

Vs. (%)	Experiment	3DMacro	Tremuri	DIANA	3DMacro_t_0	DIANA_t_0
Experiment		+36	-30	+4	+12	-16
3DMacro			-	-23	-18	-
Tremuri				-	+63	+22
DIANA					-	-20
3DMacro_t_0						-25
DIANA_t_0						

It is also important to mention that much higher ductility is achieved in the post-peak regime in the numerical models when compared to the experimental model. This feature can also be attributed to the dynamic nature of the experimental phased loading process and its effects on the structure, which is not possible to described by the non-linear static analysis.

An idea about the influence of the geometry of the building (geometric asymmetry), both on the displacement and capacity, can be driven by the possibility provided in 3DMacro allowing the obtainment of the so called Capacity Dominium [89]. This aimed at definition of the limit states and displacement capacity [26,90]. The capacity dominium identifies the direction that has the most vulnerable behavior for the model under consideration. In order to construct the capacity dominium, angular scanning analysis is performed by applying the pushover analysis with an angle which identifies the direction of the analysis relative to the positive X direction of the global coordinate system. In this sense, considering the DMEM model with tensile strength, the capacity dominium was constructed from the individual capacity curves obtained from each analyses of the angular scanning group, as illustrated in Figure 14. The directions with a certain angle are linearly interpolated. The 3D view of the domain allows to read the base shear coefficient in Z-axis while the displacements at each direction are identified on the XY plane (Figure 14(a) and (b)). Furthermore, the contour plot illustrates the intensity of the base shear coefficient for each analysis at each step. The red color highlights the directions in which the highest base shear capacity is attained (Figure 14(c)). The plots clearly illustrate that the level of resistance and ductility is influenced by the direction of the applied load due to structural asymmetry. Furthermore, the shape of the hole represents the fragility of the structural system and allows to identify for different directions. In the present case, it is observed that the ductility and base shear resistance change significantly with respect to the direction and this is, in fact, associated to the plan asymmetry and irregular distribution of the openings.

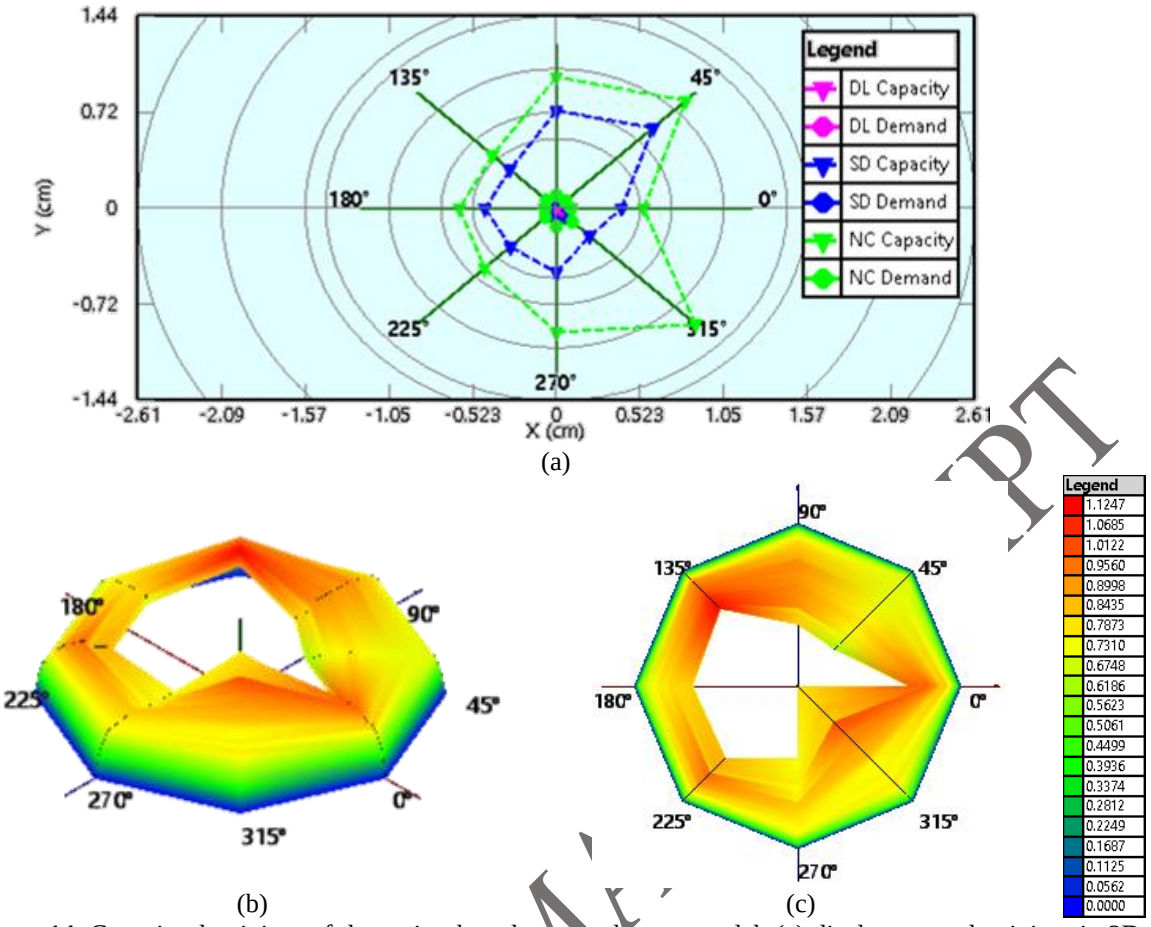

Figure 14. Capacity dominium of the spring-based macro-element model, (a) displacement dominium in 2D, (b) load factor dominium in 3D view, (c) XY plane

5.2. Damage Patterns

A critical analysis of the damage patterns is important to understand the discrepancies observed among the capacity curves obtained by the different modeling approaches and the differences between the numerical predictions and the experimental response of the building. The crack patterns under comparison correspond to the peak load recorded in each numerical model. This appears to be the most adequate solution given the different deformation levels corresponding to peak load amongst the numerical models, which are also different from the experimental model. As already mentioned, after a certain deformation level (150%, 1.07g), the large deformations recorded in the experimental model are impossible to be captured by the investigated numerical modeling strategies. Thus, the crack patterns corresponding to this seismic level is assumed to be representative of the imminent collapse.

The comparison between experimental and numerical damage patterns obtained in the continuum model and DMEM implemented in 3DMacro are presented in Figure 15 and Figure 16, respectively. In the present case, the comparison is carried out taking into account the representative models having tensile strength capacity (for continuum and macro-element models). In the case of the continuum model, the maximum principal tensile strain distribution was used to represent the model damage distribution. According to Mendes (2012) [17], the principal tensile strain distribution is a good damage indicator.

In the experimental model, the damage concentrates mostly at the first floor, even if there are some local diagonal cracks connected by long horizontal cracks developing almost along the perimeter of the building, which are believed to be the result of torsional effects of the buildings. By comparing the crack patterns obtained in both numerical models, it is observed that both reasonably describe the damage observed on the first floor. More in detail, either models (continuum and DMEM), are governed by mixed flexural (rocking) and diagonal shear mechanism. Apart from the vertical cracks observed above the openings in the spring-based macro-element model, due to the fact that the macro-model concentrates the masonry deformation at the zero-thickness interfaces, flexural (rocking) cracks developing mostly at the base of the buildings, and diagonal cracks can be seen in both models in similar regions of the structure (Figure 15 and Figure 16). It should be also noticed that the damage patterns obtained in the DMEM model are moderately influenced by the discretization of the elements.

Since the box-behavior of the structure is ensured by the rigid diaphragm, out-of-plane failure mechanisms are not expected. However, even though the structure is exposed to unidirectional lateral loading, it is possible to observe some interaction between in-plane and out-of-plane deformations, mainly at the first floor, close to the base and at the intersection of the walls (North-west intersection), as shown in Figure 16. This interaction is well captured in both numerical models, with out-of-plane deformation and horizontal cracks governed by tension failure of the North wall when the lateral load is applied in the longitudinal direction of the buildings (Y direction). This is attributed to the good (monolithic) connection assumed between longitudinal and transversal walls.

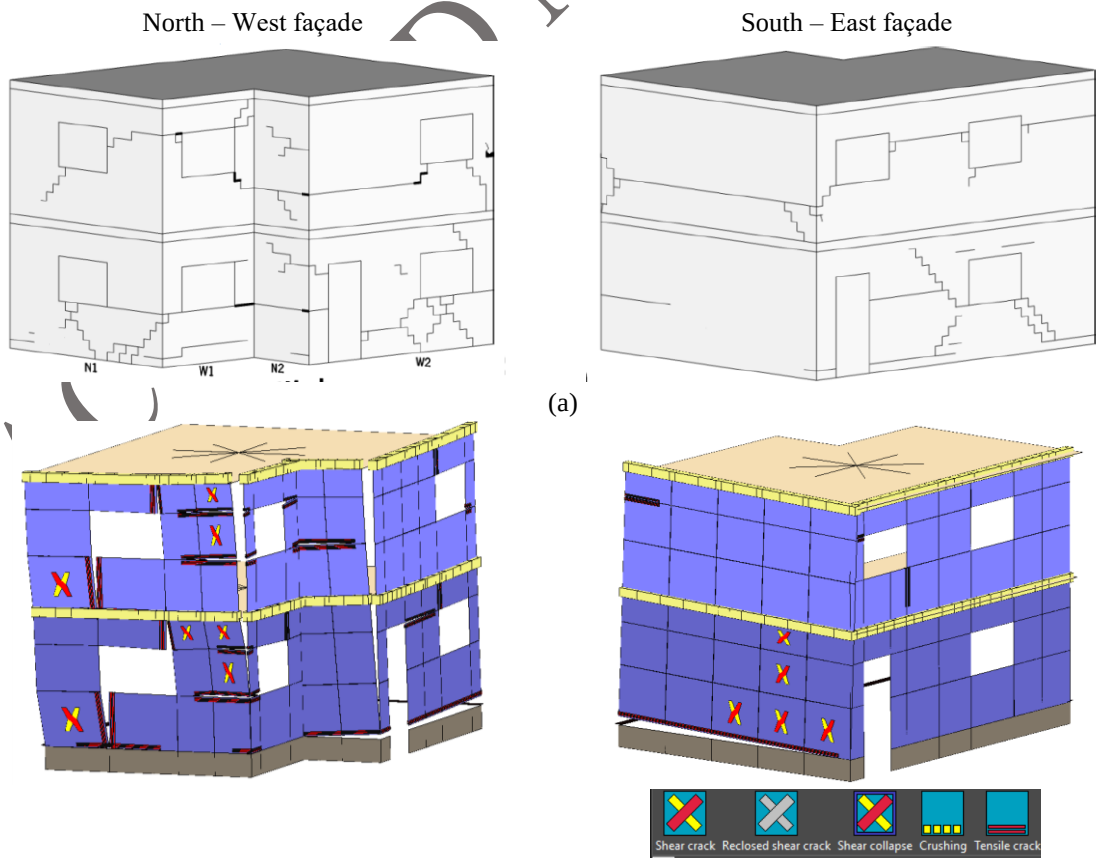

(b)

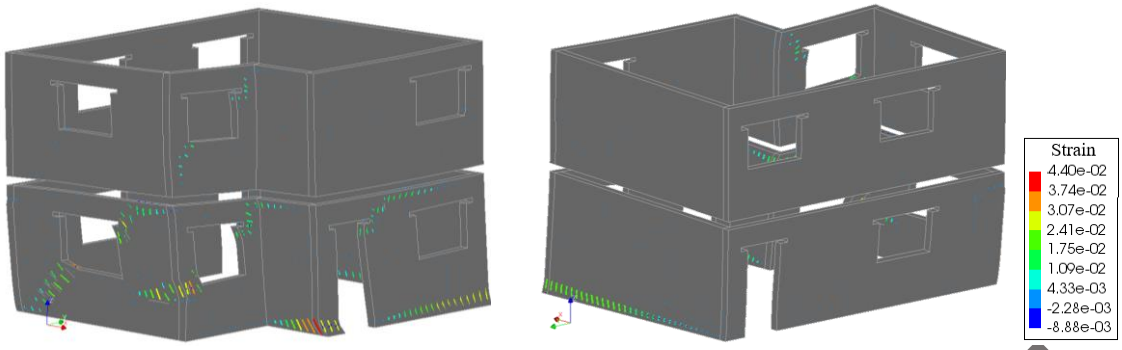

(c)

Figure 15. Damage patterns (a) at test run 150% [16]; at the peak load in -X Direction, (b) 3DMacro results for the load factor of 0.84 and displacement of 7.1 mm, (c) DIANA results for the load factor of 0.68 and displacement of 6.2 mm

In fact, the deformation and crack patterns are mostly attributed to the torsion effects of the building due to its geometry and monolithic behavior between the intersecting walls and walls and concrete slab, which was also evidenced in the experimental results as no local damages at the connections developed. It is interesting to notice that although the macro-element model only considers 2D interaction of the elements, it has the ability to capture the flexural damage due to torsional effects. Lourenço et al. (2013) [65] also stated that even regular structure tested on a shaking table presented cracks due to torsional effects resulting the asymmetric damage development in the experimental model. In general, a good agreement between the experimental and numerical results was achieved for the models, in spite of the bi-directional dynamic test.

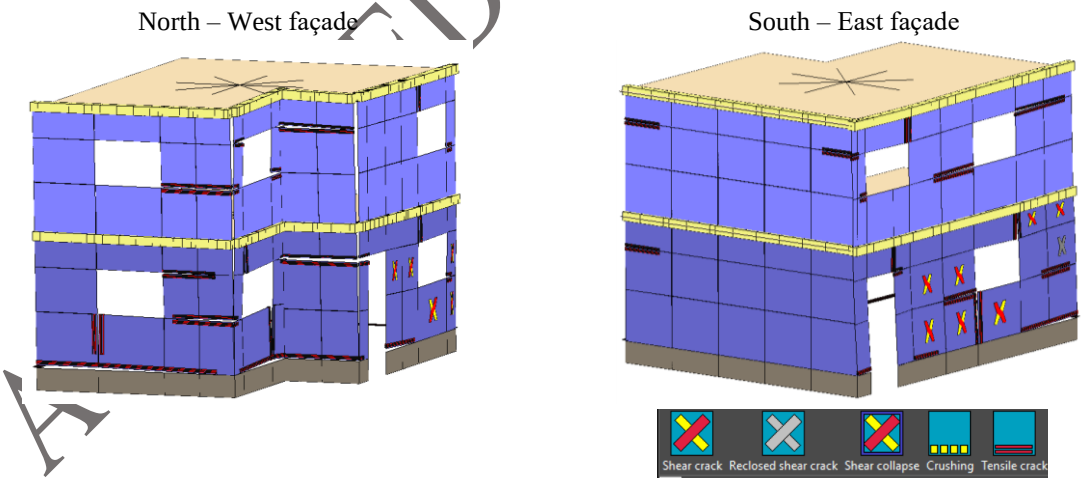

(a)

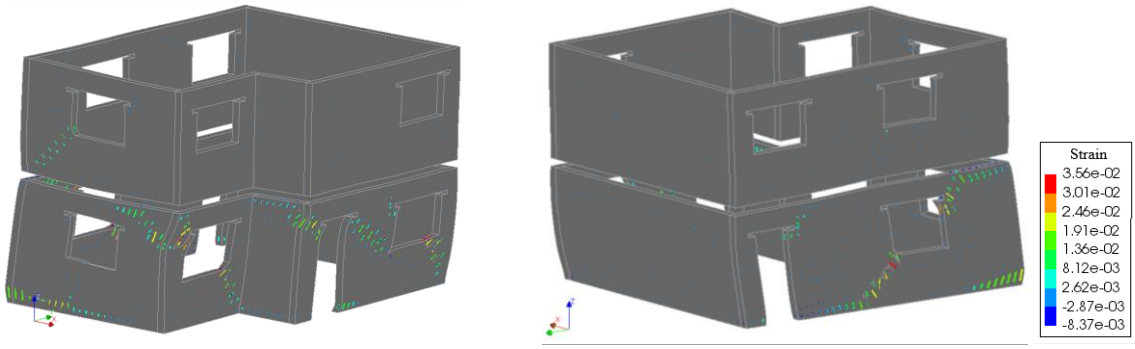

(b)

Figure 16. Damage patterns at the peak load in +Y Direction, (a) 3DMacro results for the load factor of 0.92 and displacement of 6.1 mm, (b) DIANA results for the load factor of 0.66 and displacement of 4.95 mm

The damage patterns obtained in the numerical models with zero tensile strength of masonry (FE and DMEM) are compared with the equivalent frame model implemented in Tremuri for -X and +Y direction in Figure 17 and Figure 18, respectively. In this scenario, the damage patterns have some different features regarding to previous models. In continuum element and spring-based macro-element models, mixed flexural rocking and shear cracking pattern still develop in the building under the lateral loading in the negative transversal (X) direction (Figure 17). However, in the continuum element model, there is a clear predominance of diagonal shear damage over the flexural rocking behavior. In case of the DMEM model, the zero-tensile strength of masonry favors more the flexural rocking mechanism, leading to the opening of flexural cracks at different height of the walls and to the closing of some diagonal cracks. It should be mentioned that the opening of these cracks is favored by the use of a rather large mesh of macro-elements. It is also important to note that several non-relevant vertical cracks can be identified due to the dependency of the damage on the discretization of the mesh and the nonlinear links (interfaces) with zero tensile strength between the spring-based macro-elements. This different behavior between the models should be attributed to the different constitutive material models used in each numerical model.

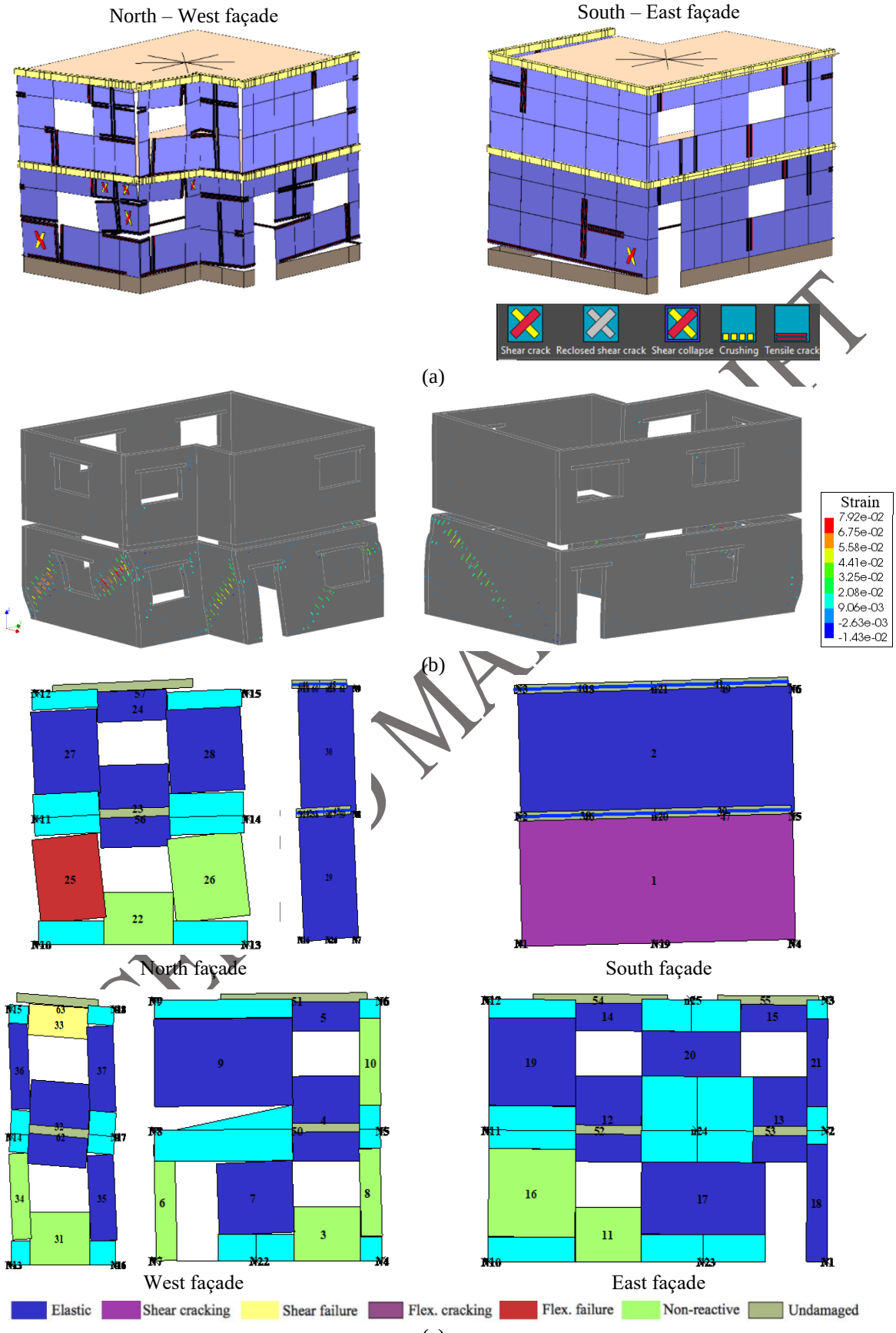

Figure 17. Damage patterns at the peak load in -X Direction, (a) 3DMacro results for the load factor of 0.69 and displacement of 11.6 mm, (b) DIANA results for the load factor of 0.48 and displacement of 12.5 mm, (c) Tremuri results for the load factor of 0.39 and displacement of 9.5 mm

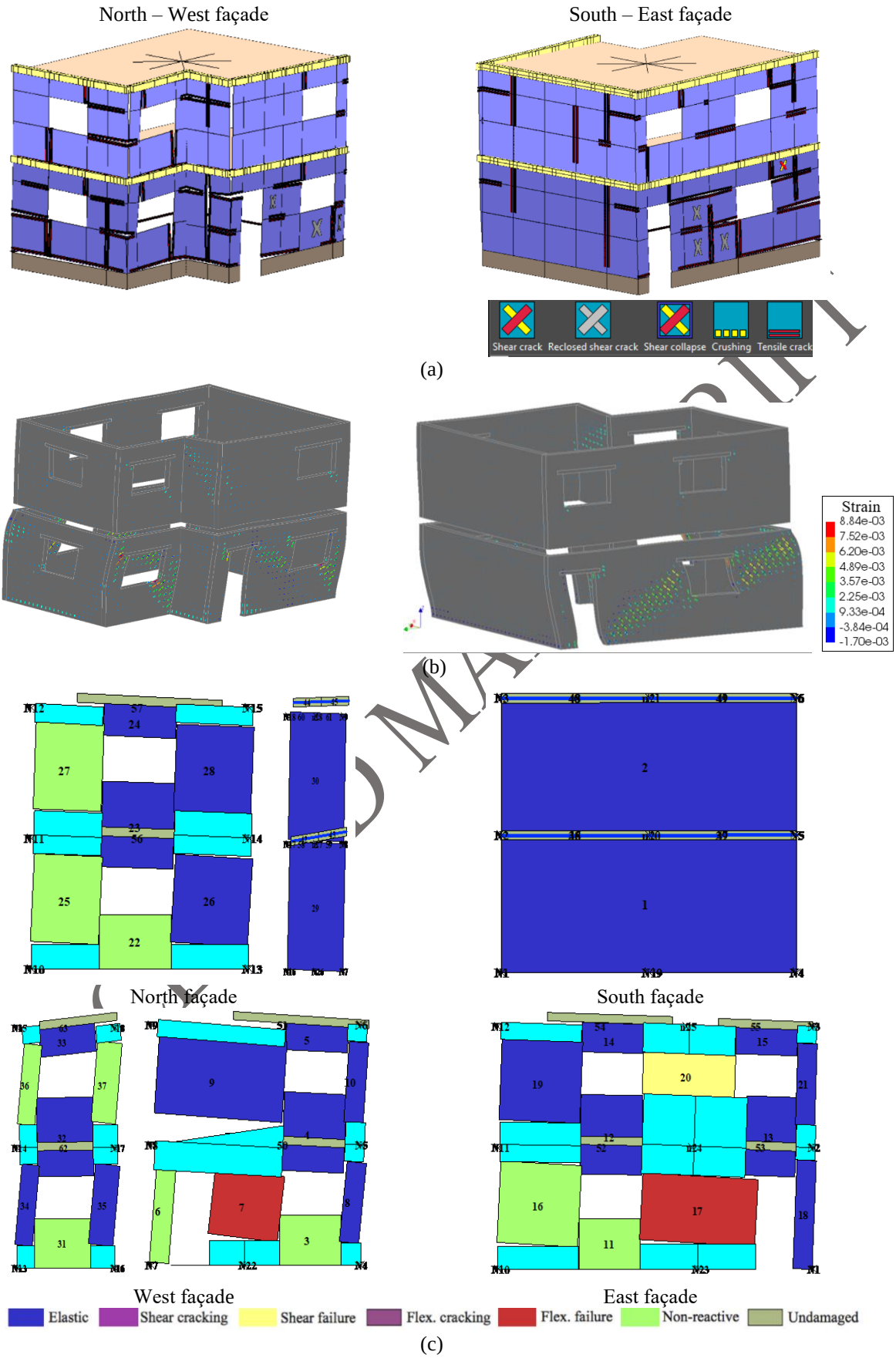

Figure 18. Damage patterns at the peak load in +Y Direction, (a) 3DMacro results for the load factor of 0.75 and displacement of 8.8mm, (b) DIANA results for the load factor of 0.55 and displacement of 2.9 mm, (c) Tremuri results for the load factor of 0.39 and displacement of 10.2 mm

It is also seen that in both numerical approaches the damage observed on the second level reduces in comparison to the models with finite tensile strength. In addition, the interaction between orthogonal walls appears to reduce, which is particularly evident in the continuum model, due to the reduction of the effectiveness of the connections at intersecting walls and thus to the lower influence of the "flange" effects in the in-plane behavior of the walls. Regarding the results obtained in the beam-based macro-element model, it is seen that the global response is governed by flexural behavior in which in-plane walls present a rocking mechanism concentrated on the North and South façades on the first floor. In this regard, the significant difference in the load capacity presented in Table 10 can be attributed to the different resisting mechanism characterizing the global behavior of the building, resulting in different numerical damage patterns. Similar to the other numerical models, the major damage concentrates on the first level.

The representative models subjected to lateral loading in the longitudinal (+Y) direction have limited agreement in terms of damage patterns as shown in Figure 18. Again, combined flexural and diagonal shear failure can be seen in the 3DMacro model. In fact, tensile cracks are not only observed at the bottom of the in-plane and out-of-plane walls but also along with the pier elements. On the other hand, the crack propagation on the continuum model shows dominant smeared diagonal shear damage along the in-plane walls. In addition, North and West façades are exposed to tensile cracks which are characterized by flexural failure. Even though the North wall is an out-of-plane wall in the longitudinal direction, a moderate horizontal crack is observed at the bottom of the structural element, which results naturally from the good connection between intersecting walls and rigid diaphragm. The equivalent frame model in Tremuri (beam-based macro-element model) presents relatively more compatible damage patterns with the continuum model in terms of flexural failure. In-plane walls exhibit flexural failure at piers on the first floor while shear failure is also noted on the pier on the second level.

6. CONCLUSIONS

The present paper is focused on the seismic performance assessment of unreinforced masonry buildings with structural irregularities in plan and elevation by means of nonlinear static analysis. The building typology was selected regarding the residential building stock to replicate typical geometry. The main motivation is to understand structural irregularity effects on the seismic response of different modeling approaches. Even if continuum modeling approach is usually accepted as an accurate numerical approach for the seismic assessment of masonry buildings, its application in engineering practice is limited due to huge computational efforts and more simplified approaches are required. Thus, promising simplified methodologies have been developed in the literature to perform structural assessment and design of masonry buildings. Such developments are crucial to promote the construction of low- to mid-rise URM buildings in seismic prone zone supported by a reliable seismic design.

Within this scope, pushover analysis of an irregular concrete block masonry building tested in a shaking table was carried out by using three different approaches, being one advanced and two

simplified, namely continuum model, spring-based macro-element and beam-based model, i.e. equivalent frame model. In order to validate the implemented methodologies, the envelop curve of the hysteretic response obtained from a dynamic shaking table test was used.

From the comparison of the results, multiple conclusions are stated as follows,

- The simplified approaches are less demanding, and, therefore, they are practical to apply in engineering practice.
- The modulus of elasticity required for the modeling approaches has to be adjusted taking into account the modeling particularities of each numerical model. This poses questions on the reliability of displacement-based seismic assessment approaches for irregular masonry buildings, given their higher dependency on elastic properties.
- Some inconsistency was found between the vibration modes in the different models, particularly in case of the torsional ones. This poses questions on the reliability of the different approaches for time history analysis of irregular masonry buildings, as the dynamic characteristics of the approaches are quite different.
- Given the important torsional components found, the mode-proportional distribution of inertial forces in case of irregular buildings should not be used. In case of pushover analyses of irregular masonry buildings, which is questionable but may be the only available tool for professionals, only uniform and inverted triangle mass distributions should be used.
- Considering masonry tensile strength, it was observed that the results from the continuum model approached relatively well the experimental envelop, being the average difference of 4% considering all directions. The simplified model built-in 3DMacro software provided, in general, higher values when compared to experimental results.
- When the tensile strength of masonry was considered to be equal to zero in the 3DMacro and Diana model, the maximum capacity was closer to the experimental response.
- The Tremuri model appeared to be excessively conservative as the maximum capacity of the building was considerably lower than the experimental load capacity. Compared to the 3DMacro and Diana model, with zero-tensile strength, the Tremuri model registered lower maximum capacity.
- A reasonable agreement was found between experimental and numerical failure modes. Some horizontal cracks developed on the second level in the experimental models, could not be found in the numerical models.
- Torsional effects were obtained on the continuum and spring-based macro-element model in which combined rocking and diagonal shear failure mechanisms was observed. This highlights the relevance of the good connections between intersecting walls and between walls and the

rigid reinforced concrete slabs. The equivalent frame model has limitations to capture damage due to torsion.

ACKNOWLEDGEMENTS

The first author acknowledges the financial support from the Portuguese Foundation for Science and Technology (FCT) through the Ph.D. Grant SFRH/BD/143949/2019. This work is financed by national funds through FCT, in the scope of the research project "Experimental and Numerical Pushover Analysis of Masonry Buildings (PUMA) (PTDC/ECI-EGC/29010/2017).

REFERENCES

[1] Jaiswal K, Wald D, Porter K. A global building inventory for earthquake loss estimation and risk management. Earthq Spectra 2010;26:731–48. doi:10.1193/1.3450316.

[2] Maio R, Ferreira TM, Estêvão JMC, Pantò B, Caliò I, Vicente R. Seismic performance-based assessment of urban cultural heritage assets through different macroelement approaches. J Build Eng 2020;29. doi:10.1016/j.jobe.2019.101083.

[3] Greco A, Lombardo G, Pantò B, Famà A. Seismic Vulnerability of Historical Masonry Aggregate Buildings in Oriental Sicily. Int J Archit Herit 2018;00:1–24. doi:10.1080/15583058.2018.1553075.

[4] Marques R, Lourenço PB. Unreinforced and confined masonry buildings in seismic regions: Validation of macro-element models and cost analysis. Eng Struct 2014;64:52–67. doi:10.1016/j.engstruct.2014.01.014.

[5] EERI. World Housing Encyclopedia 2007. http://db.world-housing.net/.

[6] Jaiswal KS, Wald DJ. Creating a Global Building Inventory for Earthquake Loss Assessment and Risk Management: U.S. Geological Survey Open-File Report 2008;1160:113.

[7] Lourenço PB, Mendes N, Ramos LF, Oliveira D V. Analysis of masonry structures without box behavior. Int J Archit Herit 2011;5:369–82. doi:10.1080/15583058.2010.528824.

[8] Betti M, Galano L, Vignoli A. Comparative analysis on the seismic behaviour of unreinforced masonry buildings with flexible diaphragms. Eng Struct 2014;61:195–208. doi:10.1016/j.engstruct.2013.12.038.

[9] Nakamura Y, Derakhshan H, Magenes G, Michael C, Nakamura Y, Derakhshan H, et al. Influence of Diaphragm Flexibility on Seismic Response of Unreinforced Masonry Buildings Influence of Diaphragm Flexibility on Seismic Response of Unreinforced Masonry Buildings 2017;2469. doi:10.1080/13632469.2016.1190799.

[10] Scotta R, Trutalli D, Marchi L, Pozza L. Seismic performance of URM buildings with in-plane non-sti ff ened and sti ff ened timber fl oors. Eng Struct 2018;167:683–94. doi:10.1016/j.engstruct.2018.02.060.

[11] Magenes G, Calvi GM, Kingsley GR. Seismic Testing of a Full-Scale, Two-Story Masonry

723 Building: Test Procedure and Measured Experimental Response. Experimental and Numerical
724 Investigation on a brick Masonry Building Prototype – Numerical Prediction of the Experiment
725 1995.
726 [12] Avila L, Vasconcelos G, Lourenço PB. Experimental seismic performance assessment of
727 asymmetric masonry buildings. Eng Struct 2018;155:298–314.
728 doi:10.1016/j.engstruct.2017.10.059.
729 [13] Azizi-Bondarabadi H, Mendes N, Lourenço PB. Higher Mode Effects in Pushover Analysis of
730 Irregular Masonry Buildings. J Earthq Eng 2019;0:1–35. doi:10.1080/13632469.2019.1579770.
731 [14] Yi T, Moon FL, Leon RT, Kahn LF. Lateral Load Tests on a Two-Story Unreinforced Masonry
732 Building. J Struct Eng 2006;132:643–52. doi:10.1061/(asce)0733-9445(2006)132:5(643).
733 [15] Graziotti F, Tomassetti U, Kallioras S, Penna A, Magenes G. Shaking table test on a full scale
734 URM cavity wall building. Bull Earthq Eng 2017;15:5329–64. doi:10.1007/s10518-017-0185-8.
735 [16] Avila L. Seismic behavior of concrete block masonry buildings. PhD Thesis, University of
736 Minho, 2014.
737 [17] Mendes N. Seismic Assessment of Ancient Masonry Buildings : Shaking Table Tests and
738 Numerical Analysis. PhD Thesis, University of Minho, 2012.
739 [18] Lourenço PB, Mendes N, Marques R. Earthquake design and assessment of masonry structures:
740 review and applications. Earthq Des Assess Mason Struct Rev Appl 2009:77–101.
741 doi:10.4203/csets.22.4.
742 [19] Lagomarsino S, Cattari S. PERPETUATE guidelines for seismic performance-based assessment
743 of cultural heritage masonry structures. Bull Earthq Eng 2015;13:13–47. doi:10.1007/s10518-
744 014-9674-1.
745 [20] Chácara C, Cannizzaro F, Pantò B, Caliò I, Lourenço PB. Seismic vulnerability of URM
746 structures based on a Discrete Macro-Element Modeling (DMEM) approach. Eng Struct
747 2019;201:109715. doi:10.1016/j.engstruct.2019.109715.
748 [21] Fajfar P. A Nonlinear Analysis Method for Performance-Based Seismic Design. Earthq Spectra
749 2000;16:573–92. doi:10.1193/1.1586128.
750 [22] Priestley MJN, Grant DN, Blandon CA. Direct displacement-based seismic design. NZSEE
751 Conf., 2005. doi:10.1016/S0141-0296(01)00048-7.
752 [23] Fajfar P, Marusic D, Perus I. Torsional Effects in the Pushover-Based Seismic Analysis of
753 Buildings. J Earthq Eng 2011;9:831–54. doi:10.1080/13632460509350568.
754 [24] Kreslin M, Fajfar P. The extended N2 method considering higher mode effects in both plan and
755 elevation. Bull Earthq Eng 2012;10:695–715. doi:10.1007/s10518-011-9319-6.
756 [25] De Stefano M, Mariani V. Pushover Analysis for Plan Irregular Building Structures. In: Ansal
757 A, editor. Perspect. Eur. Earthq. Eng. Seismol., 2014.
758 [26] Chácara C, Cannizzaro F, Pantò B, Caliò I, Lourenço PB. Seismic vulnerability of URM
759 structures based on a Discrete Macro-Element Modeling (DMEM) approach. Eng Struct

760 2019;201:109715. doi:10.1016/j.engstruct.2019.109715.
761 [27] Aşıkoğlu A, Avşar Ö, Lourenço PB, Silva LC. Effectiveness of seismic retrofitting of a historical
762 masonry structure: Kütahya Kurşunlu Mosque, Turkey. Bull Earthq Eng 2019.
763 doi:10.1007/s10518-019-00603-6.
764 [28] Ciocci MP, Sharma S, Lourenço PB. Engineering simulations of a super-complex cultural
765 heritage building: Ica Cathedral in Peru. Meccanica 2018;53:1931–58.
766 [29] Karanikoloudis G, Lourenço PB. Structural assessment and seismic vulnerability of earthen
767 historic structures. Application of sophisticated numerical and simple analytical models. Eng
768 Struct 2018;160:488–509.
769 [30] Mendes N, Lourenco PB. Seismic assessment of masonry Gaioleiro buildings in Lisbon,
770 Portugal. J Earthq Eng 2010;14:80–101. doi:10.1080/13632460902977474.
771 [31] Ramírez R, Mendes N, Lourenço PB. Diagnosis and Seismic Behavior Evaluation of the Church
772 of São Miguel de Refojos (Portugal). Buildings 2019;9:138. doi:10.3390/buildings9060138.
773 [32] Silva LC, Mendes N, Lourenço PB, Ingham J. Seismic Structural Assessment of the Christchurch
774 Catholic Basilica, New Zealand. Structures 2018;15:115–30. doi:10.1016/j.istruc.2018.06.004.
775 [33] Baraldi D, Cecchi A. A full 3D rigid block model for the collapse behaviour of masonry walls.
776 Eur J Mech A/Solids 2017;64:11–28. doi:10.1016/j.euromechsol.2017.01.012.
777 [34] D'Altri AM, de Miranda S, Castellazzi G, Sarhosis V. A 3D detailed micro-model for the in-
778 plane and out-of-plane numerical analysis of masonry panels. Comput Struct 2018;206:18–30.
779 doi:10.1016/j.compstruc.2018.06.007.
780 [35] Portioli F, Casapulla C, Gilbert M, Cascini L. Limit analysis of 3D masonry block structures
781 with non-associative frictional joints using cone programming. Comput Struct 2014;143:108–
782 21. doi:10.1016/j.compstruc.2014.07.010.
783 [36] Milani G. 3D upper bound limit analysis of multi-leaf masonry walls. Int J Mech Sci
784 2008;50:817–36. doi:10.1016/j.ijmecsci.2007.11.003.
785 [37] Lourenço PB, Rots JG. Multisurface interface model for analysis of masonry structures. J Eng
786 Mech 1997;123:660–8. doi:10.1061/(ASCE)0733-9399(1997)123:7(660).
787 [38] Chisari C, Macorini L, Amadio C, Izzuddin BA. Identification of mesoscale model parameters
788 for brick-masonry. Int J Solids Struct 2018;146:224–40. doi:10.1016/j.ijsolstr.2018.04.003.
789 [39] Silva LC, Lourenço PB, Milani G. Numerical homogenization-based seismic assessment of an
790 English-bond masonry prototype: structural level application. Earthq Eng Struct Dyn 2020:1–
791 22. doi:10.1002/eqe.3267.
792 [40] Lemos J V. Discrete element modeling of masonry structures. Int J Archit Herit 2007;1:190–
793 213. doi:10.1080/15583050601176868.
794 [41] Caliò I, Marletta M, Pantò B. A new discrete element model for the evaluation of the seismic
795 behaviour of unreinforced masonry buildings. Eng Struct 2012;40:327–38.
796 doi:10.1016/j.engstruct.2012.02.039.

[42] 3DMacro. (computer program for the seismic assessment of masonry buildings), Release 3.0, Gruppo Sismica s.r.l. 2014.

[43] Lagomarsino S, Penna A, Galasco A, Cattari S. TREMURI program: An equivalent frame model for the nonlinear seismic analysis of masonry buildings. Eng Struct 2013;56:1787–99. doi:10.1016/j.engstruct.2013.08.002.

[44] Marino S, Cattari S, Lagomarsino S, Dizhur D, Ingham JM. Post-earthquake Damage Simulation of Two Colonial Unreinforced Clay Brick Masonry Buildings Using the Equivalent Frame Approach. Structures 2019;19:212–26. doi:10.1016/j.istruc.2019.01.010.

[45] Lagomarsino S, Camilletti D, Cattari S, Marino S. Seismic assessment of existing irregular masonry buildings by nonlinear static and dynamic analyses. Geotech Geol Earthq Eng 2018;46:123–51. doi:10.1007/978-3-319-75741-4_5.

[46] Penna A, Senaldi IE, Galasco A, Magenes G. Numerical Simulation of Shaking Table Tests on Full-Scale Stone Masonry Buildings. Int J Archit Herit 2016;10:146–63. doi:10.1080/15583058.2015.1113338.

[47] Bracchi S, Penna A, Magenes G. Consideration of modelling uncertainties in the seismic assessment of masonry buildings by equivalent-frame approach. Bull Earthq Eng 2015:3423–48. doi:10.1007/s10518-015-9760-z.

[48] Bartoli G, Betti M, Biagini P, Borghini A, Ciavattone A, Girardi M, et al. Epistemic Uncertainties in Structural Modeling : A Blind Benchmark for Seismic Assessment of Slender Masonry Towers 2017;31:1–18. doi:10.1061/(ASCE)CF.1943-5509.0001049.

[49] Cattari S, Ottonelli D, Degli S, Magenes G, Filippo C. Use of computer programs for the nonlinear seismic analysis of masonry buildings : comparison of the results obtained with different software on an actual case study Uso dei codici di calcolo per l ' analisi sismica nonlineare di edifici in muratura : con 2019:235–45.

[50] Marques R, Lourenço PB. Possibilities and comparison of structural component models for the seismic assessment of modern unreinforced masonry buildings. Comput Struct 2011;89:2079–91. doi:10.1016/j.compstruc.2011.05.021.

[51] Magenes G, Della Fontana A. Simplified Non-Linear Seismic Analysis of Masonry Buildings. Proc Br Maasonry Soc 1998:1–313. doi:10.6092/UNINA/FEDOA/8417.

[52] Pantò B, Cannizzaro F, Caliò I, Lourenço PB. Numerical and Experimental Validation of a 3D Macro-Model for the In-Plane and Out-Of-Plane Behavior of Unreinforced Masonry Walls. Int J Archit Herit 2017;11:946–64. doi:10.1080/15583058.2017.1325539.

[53] Chácara E. CJ. Macro-Element Nonlinear Dynamic Analysis for the Assessment of the Seismic Vulnerability of Masonry Structures. 2018:1–173.

[54] Bondarabadi HA. Analytical and empirical seismic fragility analysis of irregular URM buildings with box behavior. University of Minho, 2018.

[55] D'Altri A, Sarhosis V, Milani G, Rots J, Cattari S, Lagomarsino S, et al. Modeling Strategies for

the Computational Analysis of Unreinforced Masonry Structures: Review and Classification. Arch Comput Methods Eng 2019. doi:10.1007/s11831-019-09351-x.

[56] Theodossopoulos D, Sinha B. A review of analytical methods in the current design processes and assessment of performance of masonry structures. Constr Build Mater 2013;41:990–1001. doi:10.1016/j.conbuildmat.2012.07.095.

[57] Tomaževič M. Earthquake-Resistant Design of Masonry Building. London: Imperial College Press; 1999.

[58] Calderini C, Cattari S, Lagomarsino S. In-plane strength of unreinforced masonry piers. Earthq Eng Struct Dyn 2009;38:243–67. doi:10.1002/eqe.860.

[59] Betti M, Galano L, Petracchi M, Vignoli A. Diagonal cracking shear strength of unreinforced masonry panels: a correction proposal of the b shape factor. Bull Earthq Eng 2015;13:3151–86. doi:10.1007/s10518-015-9756-8.

[60] Tomaževič M. The computer program POR. Report ZRMK 1978.

[61] D'Asdia P, Viskovic A. Analyses of a masonry wall subjected to horizontal actions on its plane, employing a non-linear procedure using changing shape finite element. Trans Model Simul 1995;10:519–26. doi:10.2495/CMEM950571.

[62] Braga F, Liberatore D. A finite element for the analysis of the response of masonry buildings. 5th North Am. Mason. Conf., Urbana: 1990, p. 201–12.

[63] Foraboschi P, Vanin A. Non-linear static analysis of masonry buildings based on a strut-and-tie modeling. Soil Dyn Earthq Eng 2013;55:44–58. doi:10.1016/j.soildyn.2013.08.005.

[64] Braga F, Liberatore D, Spera G. A computer program for the seismic analysis of complex masonry buildings. Comput. Methods Struct. Mason. - 4th Int. Symp., Firenze: 1997, p. 309–16.

[65] Lourenço PB, Avila L, Vasconcelos G, Alves JPP, Mendes N, Costa AC. Experimental investigation on the seismic performance of masonry buildings using shaking table testing. Bull Earthq Eng 2013;11:1157–90. doi:10.1007/s10518-012-9410-7.

[66] Eurocode 8. EN 1998-1: Design of structures for earthquake resistance - Part 1: General rules, seismic actions and rules for buildings 2004.

[67] Carvalho E. Seismic testing of structures. Earthq Eng Pap Proc Elev Eur Conf 1999;2:53.

[68] Eurocode 8. Design of structures for earthquake resistancepart 3: Assessment and retrofitting of buildings 2005.

[69] Lourenço PB. Computations on historic masonry structures. Prog Struct Eng Mater 2002;4:301–19. doi:10.1002/pse.120.

[70] Chácara C, Lourenço PB, Pantò B, Cannizzaro F, Caliò I. Parametric numerical studies on the dynamic response of unreinforced masonry structures. Struct Anal Hist Constr Anamn Diagnosis, Ther Control - Proc 10th Int Conf Struct Anal Hist Constr SAHC 2016 2016:239–45. doi:10.1201/9781315616995-30.

[71] Pantò B, Giresini L, Sassu M, Caliò I. Non-linear modeling of masonry churches through a

discrete macro-element approach. Earthq Struct 2017;12:223–36. doi:10.12989/eas.2017.12.2.223.

[72] Magenes G, Calvi GM. Cyclic behavior of brick masonry walls. 10th World Conf. Earthq. Eng., Rotterdam: 1992, p. 3517–22.

[73] Vasconcelos GFM. Experimental investigations on the mechanics of stone masonry: Characterization of granites and behavior of ancient masonry shear walls. PhD Thesis 2005:266.

[74] Araújo A. Modelling of the Seismic Performance of Connections and Walls in Ancient Masonry Buildings. PhD Thesis, University of Minho, 2014.

[75] Petry S, Beyer K. Influence of boundary conditions and size effect on the drift capacity of URM walls. Eng Struct 2014;65:76–88. doi:10.1016/j.engstruct.2014.01.048.

[76] Simões A. Evaluation of the seismic vulnerability of the unreinforced masonry buildings constructed in the transition between the 19 th and 20 th centuries in Lisbon, Portugal. PhD Thesis, Universidade de Lisboa Instituto Superior Tecnico, 2018.

[77] Magenes G, Penna A, Galasco A, da Paré M. In-plane cyclic shear tests of undressed double leaf stone masonry panels. 8th Int Masorny Conf 2010:1–10.

[78] Lagomarsino S, Penna A, Galasco A. TREMURI program: seismic analysis program for 3D masonry buildings. Univ Genoa 2006.

[79] DIANA FEA. User's Manual Release 10.2 2017.

[80] Angelillo M, Lourenço P, Milani G. Masonry behavior and modelling. In: Angelillo M, editor. Mech. Mason. Struct., Udine: CISM International Centre for Mechanical Sciences, Springer; 2014, p. 1–24.

[81] Gambarotta L, Lagomarsino S. Damage Models for the seismic response of brck masonry shear walls. Part II: the continuum model and its applications. Earthq Eng Struct Dyn 1997;26:441–62.

[82] Penna A, Lagomarsino S, Galasco A. A nonlinear macroelement model for the seismic analysis of masonry buildings. Earthq Eng Struct Dyn 2014;43:159–79.

[83] Pantò B, Cannizzaro F, Caliò I, Lourenço PB. Numerical and Experimental Validation of a 3D Macro-Model for the In-Plane and Out-Of-Plane Behavior of Unreinforced Masonry Walls. Int J Archit Herit 2017;11:946–64. doi:10.1080/15583058.2017.1325539.

[84] Mann W, Muller H. Failure of shear-stressed masonry. An enlarged theory, tests and application to shear walls. Proc Br Ceram Soc 1982:223.

[85] Eurocode 6. Design of masonry structures - Part 1-1: General rules for reinforced and unreinforced masonry structures. 2005.

[86] Gruppo Sismica. 3DMacro - Manuale Teorico 2013.

[87] Lagomarsino S, Penna A, Galasco A, Cattari S. TREMURI program: seismic analyses of 3D masonry buildings 2012.

[88] Siano R, Sepe V, Camata G, Spacone E, Roca P, Pelà L. Analysis of the performance in the

linear field of Equivalent-Frame Models for regular and irregular masonry walls. Eng Struct 2017;145:190–210. doi:10.1016/j.engstruct.2017.05.017.

[89] Caliò I, Cannizzaro F, D'Amore E, Marletta M, Pantò B. A new discrete-element approach for the assessment of the seismic resistance of composite reinforced concrete-masonry buildings. AIP Conf Proc 2008;1020:832–9. doi:10.1063/1.2963920.

[90] Cannizzaro F, Pantò B, Lepidi M, Caddemi S, Caliò I. Multi-directional seismic assessment of historical masonry buildings by means of macro-element modelling: Application to a building damaged during the L'Aquila earthquake (Italy). Buildings 2017;7:1–24. doi:10.3390/buildings7040106.